NASA CONTRACTOR REPORT
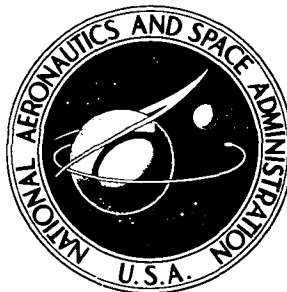
NASA CR-2440

NASA CR-2440

VISCOSITY AND THERMAL CONDUCTIVITY COEFFICIENTS OF GASEOUS AND LIQUID OXYGEN

by H. J. M. Hanley, R. D. McCarty, and J. V. Sengers

Prepared by
UNIVERSITY OF MARYLAND
College Park, Md. 20742
for Lewis Research Center

NATIONAL AERONAUTICS AND SPACE ADMINISTRATION • WASHINGTON, D. C. • AUGUST 1974

1. Report No. NASA CR-2440	2. Government Accession No.	3. Recipient's Catalog No.
4. Title and Subtitle VISCOSITY AND THERMAL CONDUCTIVITY COEFFICIENTS OF GASEOUS AND LIQUID OXYGEN		5. Report Date August 1974
		6. Performing Organization Code
7. Author(s) H. J. M. Hanley, R. D. McCarty, National Bureau of Standards, Boulder, Colorado; and J. V. Sengers, University of Maryland		8. Performing Organization Report No. None
		10. Work Unit No.
9. Performing Organization Name and Address University of Maryland College Park, Maryland 20742		
		11. Contract or Grant No. NGL-21-002-344
		13. Type of Report and Period Covered Contractor Report
12. Sponsoring Agency Name and Address National Aeronautics and Space Administration Washington, D.C. 20546		
		14. Sponsoring Agency Code

15. Supplementary Notes

Final Report. Project Manager, Robert J. Simoneau, Physical Science Division, NASA Lewis Research Center, Cleveland, Ohio

16. Abstract

The report presents equations and tables for the viscosity and thermal conductivity coefficients of gaseous and liquid oxygen at temperatures between 80 K and 400 K for pressures up to 200 atm. and at temperatures between 80 K and 2000 K for the dilute gas. A description of the anomalous behavior of the thermal conductivity in the critical region is included. The tabulated coefficients are reliable to within about 15% except for a region in the immediate vicinity of the critical point. Some possibilities for future improvements of this reliability are discussed.

17. Key Words (Suggested by Author(s)) Correlation length; Critical phenomena; Intermolecular potential; Oxygen; Thermal conductivity; Transport properties; Viscosity	18. Distribution Statement Unclassified - unlimited Category 33	
19. Security Classif. (of this report) Unclassified	20. Security Classif. (of this page) Unclassified	21. No. of Pages 77	22. Price* $4.00

TABLE OF CONTENTS

LIST OF TABLES

LIST OF FIGURES

I. Introduction

The present technical report is concerned with the viscosity and thermal conductivity of oxygen over a wide range of temperatures and pressures including temperatures and pressures close to that of the critical point. The experimental information available for the transport properties of oxygen is summarized in Section II. Unfortunately, this experimental information is of limited scope and reliability. As a result it is difficult to produce authorative tables of the transport properties of oxygen covering a wide range of temperatures and pressures. Therefore, any tabulation of the transport properties of oxygen at this time must be based on estimated values and will be subject to revisions as further experimental data and better methods for predicting and correlating transport properties will become available.

For most technological applications it is desirable to represent the transport properties as a function of the pressure P and the temperature T of the fluid and we shall indeed present tables of transport properties in terms of these variables. However, in order to produce such tables it is convenient, if not necessary, to analyze the transport properties in terms of the density ρ and the temperature T of the fluid [1]. In doing so we decompose the viscosity, η, and the thermal conductivity, λ, into three separate contributions:

$$\eta = \eta(\rho,T) = \eta_o(T) + \Delta\eta(\rho) + \Delta_c\eta(\rho,T) , \tag{1a}$$

$$\lambda = \lambda(\rho,T) = \lambda_o(T) + \Delta\lambda(\rho) + \Delta_c\lambda(\rho,T) , \tag{1b}$$

Here, $\eta_o(T)$ and $\lambda_o(T)$ are the values of the transport coefficient at the temperature T in the limit of low pressures, $\Delta\eta(\rho)$ and $\Delta\lambda(\rho)$ are the so-called excess values which measure the enhancement of the viscosity and thermal conductivity, respectively, at a given temperature T and density

1

ρ over its dilute gas value, while $\Delta_c \eta(\rho, T)$ and $\Delta_c \lambda(\rho, T)$ represent the additional anomalous contribution in the region around the critical point. To an approximation, adequate for the purpose of this report, the excess values $\Delta\eta(\rho)$ and $\Delta\lambda(\rho)$ will be treated as a function of the density only.

The procedure is illustrated in Fig. 1 which shows schematically the thermal conductivity $\lambda(\rho, T)$ as a function of the density ρ at three temperatures $T_1 < T_2 < T_3$ above the critical temperature T_c. In an appreciable range of supercritical temperatures the thermal conductivity is known to exhibit an anomalous increase in a range of densities around the critical density ρ_c. The dilute gas value $\lambda_o(T)$ in (1b) is the value of $\lambda(\rho, T)$ in the limit $\rho \to 0$, the excess value $\Delta\lambda(\rho)$ in (1b) is the difference between the values represented by the dashed curves in Fig. 1 and $\lambda_o(T)$, and the term $\Delta_c \lambda(\rho, T)$ represent the additional contribution to be added to account for the effect of the vicinity of the critical point. In Fig. 1 we have indicated explicitly these three contributions at $\rho = \rho_c$ and $T = T_1$.

Our method for calculating the dilute gas values $\eta_o(T)$ and $\lambda_o(T)$ is based on the kinetic theory of gases and is described in Section III. The excess values $\Delta\eta(\rho)$ and $\Delta\lambda(\rho)$ will be represented by an empirical equation discussed in Section IV. A method for estimating the critical enhancement $\Delta_c \lambda(\rho, T)$ in the thermal conductivity is described in Section V. This method is based on an empirical extension of the ideas presented in a preceding NASA Contractor Report [2]. Although a critical enhancement $\Delta_c \eta(\rho, T)$ in the viscosity does exist, it is much smaller than the corresponding effect in the thermal conductivity and it will be neglected for the purpose of this report.
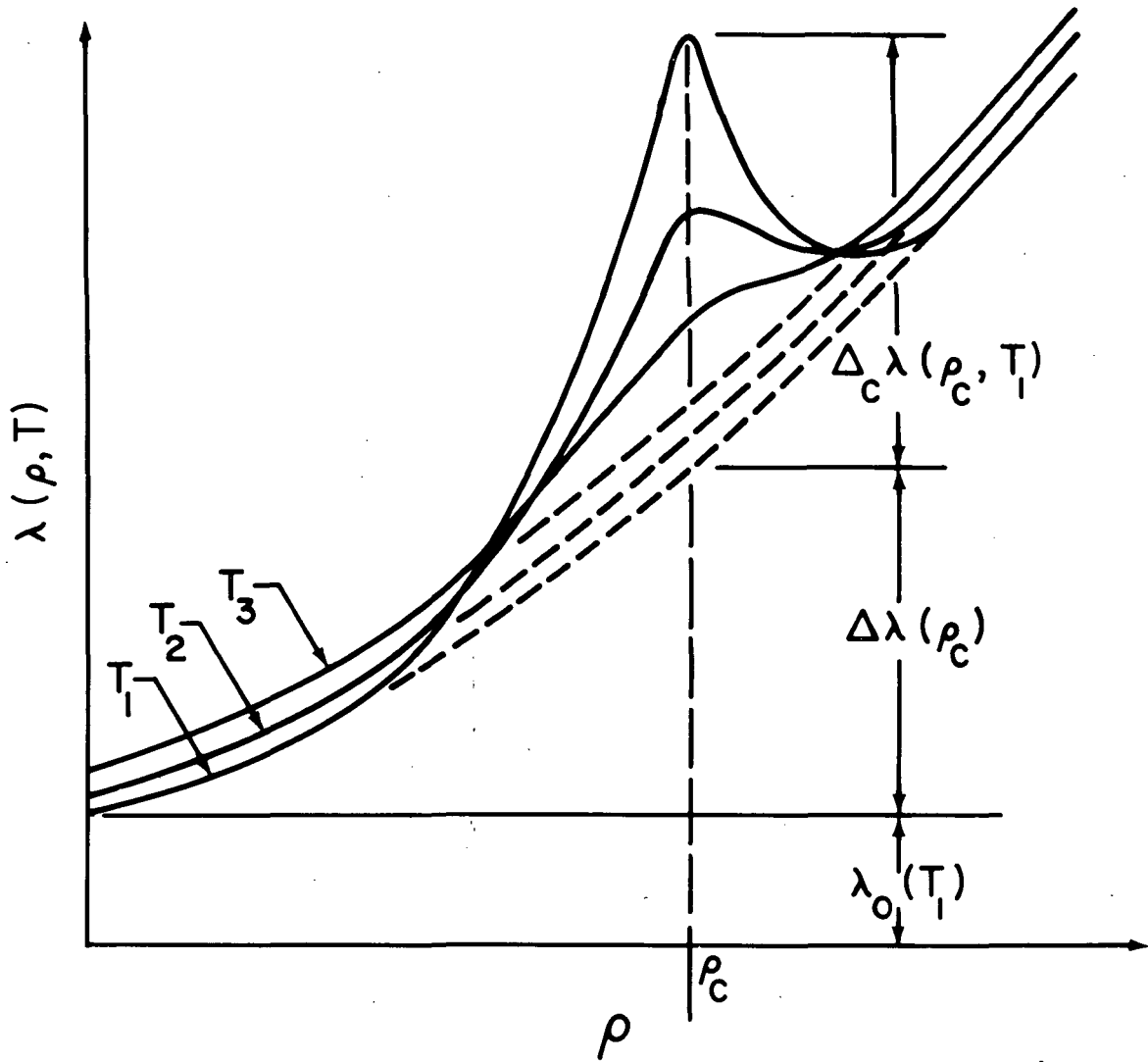
Figure 1. Schematic representation of the thermal conductivity $\lambda(\rho,T)$ as a function of the density ρ at three supercritical temperatures $T_c < T_1 < T_2 < T_3$.

In Appendices A and B we present some additional information in support of the calculation procedures used in this report.

Tables of estimated values for the viscosity and thermal conductivity of oxygen are presented in Section VI. Except for the data in the immediate vicinity of the critical point, we assign to these values an accuracy of 10-15%.

II. Experimental information.

2.1 Dilute gas

Experimental data for the viscosity of oxygen at low pressures have

been reported by several authors, specifically Wobser and Müller [3],

Kestin and Leidenfrost [4], Andrussow [5], Van Lierde [6], Johnston and

McCloskey [7], Trautz et al. [8], Raw and Ellis [9] and Van Itterbeek

and Claes [10]. The data from these sources are numerous and cover a

wide temperature range. Unfortunately, an analysis of available vis-

cosity data for many common gases other than oxygen indicates that most

of this work must be considered out of date. The state of the art for

measuring the viscosity has improved significantly since about 1967

[11-14] and it is now generally accepted that most of the earlier data

are systematically in error at temperatures below 250 K and above 400 K.

At temperatures between 400 K and 2000 K modern experiments give vis-

cosity coefficients that tend to be 1-10% larger than their older equiv-

alents, the difference increasing with temperature. At low temperatures

the discrepancy is less pronounced but the modern data are generally

1/2 - 2% below the older data, the difference increasing as the temperature

decreases.

The difference between the old and the modern data is plotted in

Fig. 2 as a function of temperature. It turns out that this difference

is almost independent of the nature of the gas and Fig. 2 is based on

available measurements for helium, argon, krypton, methane, nitrogen and

air. In order to construct this figure the older data were taken from

Trautz [15] and Johnston et al. [7,16] and the modern data from Kestin

5
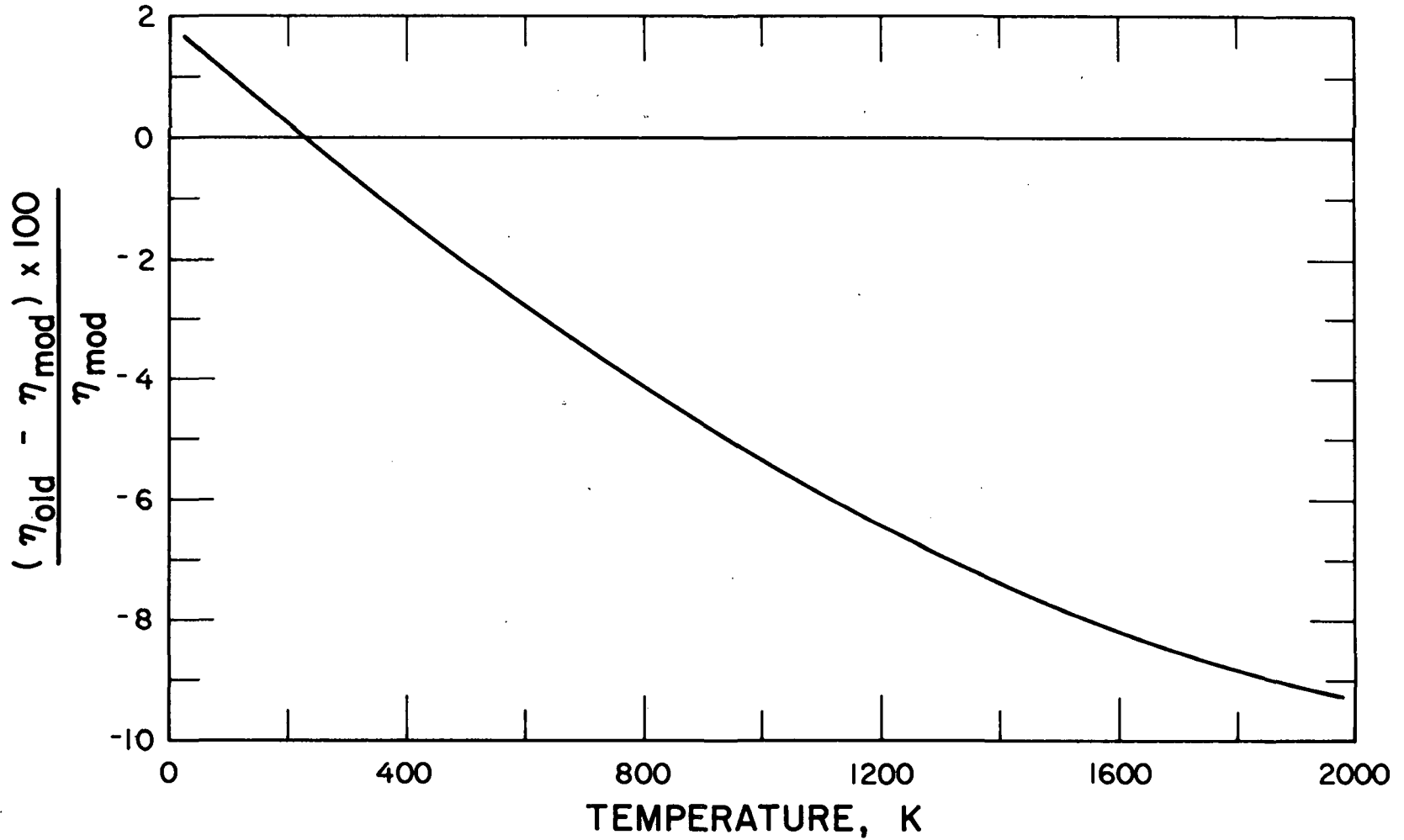
Figure 2. Difference between old and modern viscosity data for several gases as a function of temperature.

et al. [11], Smith et al. [12] and Guevara et al. [13]. For further discussions concerning this discrepancy the reader is referred to the literature [11-14].

In view of this discrepancy the viscosity data for oxygen below 250 K and above 400 K are expected to be subject to similar errors. We estimated these errors by assuming them to be the same as for the other gases and we adjusted the viscosity data of references [7-9] by the amount shown in Fig. 2. The adjusted viscosity values are listed in Table I.

Values for the thermal conductivity of oxygen have been reported by various authors [17-27]. However, due to basic difficulties in measuring the thermal conductivity coefficient, the data are imprecise and agreement between different authors is not good; even results from a single author may frequently scatter by 5% or more. However, it will be shown that kinetic theory can be used to *predict* the thermal conductivity and the data are required only to check our calculated values.

2.2 Dense gas and liquid

Viscosity data for the saturated liquid are reported in references [28-30]. At a given temperature the data sets agree to within 5-15% with the discrepancies becoming more apparent as the critical temperature is approached. Viscosity data for oxygen at liquid densities and temperatures off the saturation boundary are reported only by Grevendonk et al. [30].

Viscosity data for dense oxygen at temperatures above the critical temperature are scarce and appear to be given only in references [4] and [31]. One must conclude that, in the experimental coverage of the viscosity, gaps exist between the dilute gas and the liquid state.

7

Table I

Adjusted experimental viscosities for oxygen at low pressures.

Temperature K	Viscosity, $\eta_o(T)$ milligram/cm.s
90.3	0.0679
118.8	0.0890
131.3	0.0979
144.9	0.108
158.5	0.117
172.6	0.128
184.6	0.137
400.8	0.258
500.1	0.305
550.1	0.327
556.1	0.328
675.1	0.377
769.1	0.411
881.1	0.450
963.1	0.477
1102.1	0.521

Experimental data for the thermal conductivity of oxygen are reported by Ziebland and Burton [32], Ivanova, Tsederberg and Popov [33] and Tsederberg and Timrot [24]. The different data sets agree to within about 10%.

It has been demonstrated that the thermal conductivity of many gases exhibits an anomalous increase in a wide range of densities and temperatures around the critical point [1,2]. However, no experimental data for the thermal conductivity of oxygen in the critical region are currently available.

Some additional experimental sources are mentioned in the compilations of Childs and Hanley [34], Ho et al. [35], Maitland and Smith [36] and Vasserman et al. [37].

The many applications of oxygen in science and engineering notwithstanding, the data coverage for the viscosity and thermal conductivity coefficients of oxygen is poor. This lack of reliable data hampers the production of authorative tables of transport properties of oxygen covering a wide range of temperatures and pressures.

III. <u>Transport properties of the dilute gas</u>.

3.1 <u>Equation for viscosity</u>

In the kinetic theory of gases the viscosity coefficient $\eta_o(T)$ in equation (1a) is given by [38,39].

$$\eta_o(T) = \frac{5}{16} \frac{(\pi m k T)^{1/2}}{\pi \sigma^2 \Omega^{(2,2)*}} \tag{2}$$

where m is the weight of a molecule, k is Boltzmann's constant, and T the temperature in Kelvin. The quantity $\Omega^{(2,2)*}$ is a dimensionless collision integral which takes into account the dynamics of a binary collision and is characteristic of the intermolecular potential of the colliding molecules. For a given potential, $\Phi(r)$, with an energy parameter ϵ [defined as the value of $\Phi(r)$ at the maximum energy of attraction] $\Omega^{(2,2)*}$ can be determined as a function of the reduced temperature

$$T^* = T/(\epsilon/k) \tag{3}$$

The parameter σ is a distance parameter, also characteristic of the intermolecular potential, and is the value of r when $\Phi(r) = 0$.

For the purposes of this report we use collision integrals based on an intermolecular potential $\Phi(r)$ that is spherically symmetric. This procedure applies strictly to the noble gases only and not to a polyatomic gas like oxygen. However, it is possible to use a spherically symmetric potential to correlate the transport properties of single polyatomic gases, if one is satisfied with a precision of about 5% [40].

The specific relationship between the collision integrals $\Omega^{(\ell,s)*}$ and $\Phi(r)$ is as follows. A variable g* is defined as the reduced relative

10

kinetic energy of two colliding molecules: $g*^2 = \mu g^2 / 2\varepsilon$, where μ is the reduced mass and g the relative velocity. An impact parameter b is defined as the distance of one molecule from the direction of approach of another before collision.

With r the intermolecular separation and r_c the distance of closest approach, the angle of scatter, χ, after a collision is related to the potential by [39]

$$\chi = \pi - 2b* \int_{r_c^*}^{\infty} \frac{dr*}{r*^2} \left[1 - \frac{b*^2}{r*^2} - \frac{\Phi*}{g*^2} \right]^{-\frac{1}{2}} \tag{4}$$

where the variables are reduced according to the relations: $b* = b/\sigma$, $r* = r/\sigma$, $r_c^* = r_c/\sigma$, $\Phi* = \Phi/\varepsilon$. Integration of χ over all values of $b*$ yields the cross section, $Q*$,

$$Q^{(\ell)*} = \frac{2}{\left[1 - \frac{1}{2} \frac{(1 + (-1)^\ell)}{1 + \ell} \right]} \int_0^{\infty} (1 - \cos^\ell \chi) b* db* \tag{5}$$

[$Q^{(\ell)*}$ is dimensionless and has been reduced by the corresponding value for molecules interacting with a hard sphere potential.] Finally, integration of $Q*$ over all values of $g*$ gives

$$\Omega^{(\ell,s)*}(T*) = \frac{2}{(s+1)! \, T*^{(s+2)}} \int_0^{\infty} \exp(-g*^2/T*) g*^{(2s+3)} Q^{(\ell)*}(g*) dg* , \tag{6}$$

and $\Omega^{(2,2)*}$ follows when ℓ, s are both set equal to 2.

3.2 Equation for thermal conductivity.

In order to calculate the thermal conductivity coefficient $\lambda_o(T)$ in equation (1b) for a polyatomic gas we use the kinetic theory expression derived by Mason and Monchick [41]

$$\lambda_o(T) = \frac{15}{4}\frac{k}{m}\eta_o + \rho D_o c_v'' - \frac{2c_v}{\pi Z}\left(\frac{5}{2} - \frac{D_o}{\eta}\right)\eta_o$$

where c_v'' is the internal specific heat per molecule of the dilute gas, Z the rotational collision number (defined as the number of collisions needed to relax the rotational energy to within 1/e of its equilibrium value, where e is the natural logarithm base), and D_o a diffusion co-efficient for internal energy. In practice, D_o is approximated by the self diffusion coefficient to be obtained from

$$D_o = \frac{3}{8}\frac{(\pi mkT)^{1/2}}{\pi\sigma^2\Omega^{(1,1)*}} \qquad . \qquad (8)$$

Here $\Omega^{(1,1)*}$ is the collision integral for diffusion, given by equation (6) with ℓ,s set equal to 1. It is also noted that equation (7) has been linearized by neglecting terms in the denominator of the third term that depend on the rotational collision number Z.

3.3 Intermolecular potential function.

It is apparent from equations (2-8) that, given c_v'' and Z, the cal-culations for the viscosity and thermal conductivity coefficients are straight forward once the function $\Phi(r)$ is known. Unfortunately, obtaining $\Phi(r)$ for a fluid presenta a problem: except for the very simplest systems, $\Phi(r)$ has to be based on a model of the intermolecular interaction and so uncertainty is inevitably introduced into kinetic theory or statistical mechanical calculations. Nevertheless, model functions are often all

that one requires if they are employed carefully. For example, a
recent function, proposed by Klein and Hanley [40,42] has been found to
be very useful. The function is called an m-6-8 potential and has the
form:

$$\Phi(r)/\varepsilon = \frac{1}{m-6}\,(6+2\gamma)\left(\frac{d}{r^*}\right)^m - \frac{1}{m-6}\,\{m-\gamma(m-8)\}\left(\frac{d}{r^*}\right)^6 - \gamma\left(\frac{d}{r^*}\right)^8 \quad , \quad (9)$$

where $r^* = r/\sigma$, $d = r_m/\sigma$, r_m being the distance corresponding to the
minimum of the potential: $\Phi(r_m) = -\varepsilon$. The potential function (9) has
four parameters; in addition to ε and σ (or r_m), the potential function
contains a parameter m determining the strength of the repulsive part
and a parameter γ representing an attraction due to the presence of
the r^{*-8} term.

The basic equations (2), (7) and (9) involve several approximations
when applied to a polyatomic gas such as oxygen, the most serious of which
is that the potential function (9) is spherically symmetric. However,
we have demonstrated in earlier papers that the potential function (9)
can nevertheless be used to correlate the transport properties of simple poly-
atomic gases to within experimental error [40,43,44]. Therefore, since our
objective here is indeed to correlate transport properties, we feel
justified to employ the m-6-8 potential (9) with equations (2) and (7)
as given. Some additional information in support of this procedure is
presented in Appendix A.

3.4 Application to oxygen.

Following a procedure described in earlier publications [40,43]
the adjusted experimental viscosities listed in Table I lead to the
following parameters of the m-6-8 potential function (9):

$$m = 10, \quad \gamma = 1.0, \quad \sigma = 3.437\mathring{A} \ (r_m = 3.8896\mathring{A}), \quad \varepsilon/k = 113.0K. \qquad (10)$$

Tables of the collision integrals $\Omega^{(2,2)*}$ and $\Omega^{(1,1)*}$ as a function of T^*
are available for several values of the parameters m and γ [45]. In order
to calculate the thermal conductivity coefficient $\lambda_o(T)$ we need in addition
the internal specific heat c_v'' and the rotational collision number. The
internal specific heat c_v'' is well known and was taken from ref. [46].
The rotational collision number is less certain, but Sandler has surveyed
the methods for determining Z and concluded that, for oxygen, Z ≈ 2 at
100 K and varies smoothly to Z≈7 at 1000 K [47]. Therefore, between 100 K
and 1000 K the value of Z as a function of temperature was obtained by
interpolating between these values, while for temperatures above 1000 K
Z was set equal to 7.5. It was verified that the calculated thermal
conductivities were insensitive to the precise value assigned to Z.

Having values for c_v'', Z, ε, σ and the collision integrals, the
viscosity and thermal conductivity coefficients of dilute gaseous oxygen
were calculated from equations (2) and (7) as a function of temperature. The
differences between experimental and calculated transport coefficients
are shown in Figs. 3 and 4 for the viscosity $\eta_o(T)$ and the thermal
conductivity $\lambda_o(T)$, respectively. We regard the agreement between ex-
perimental and calculated values as satisfactory and used, therefore, this

14
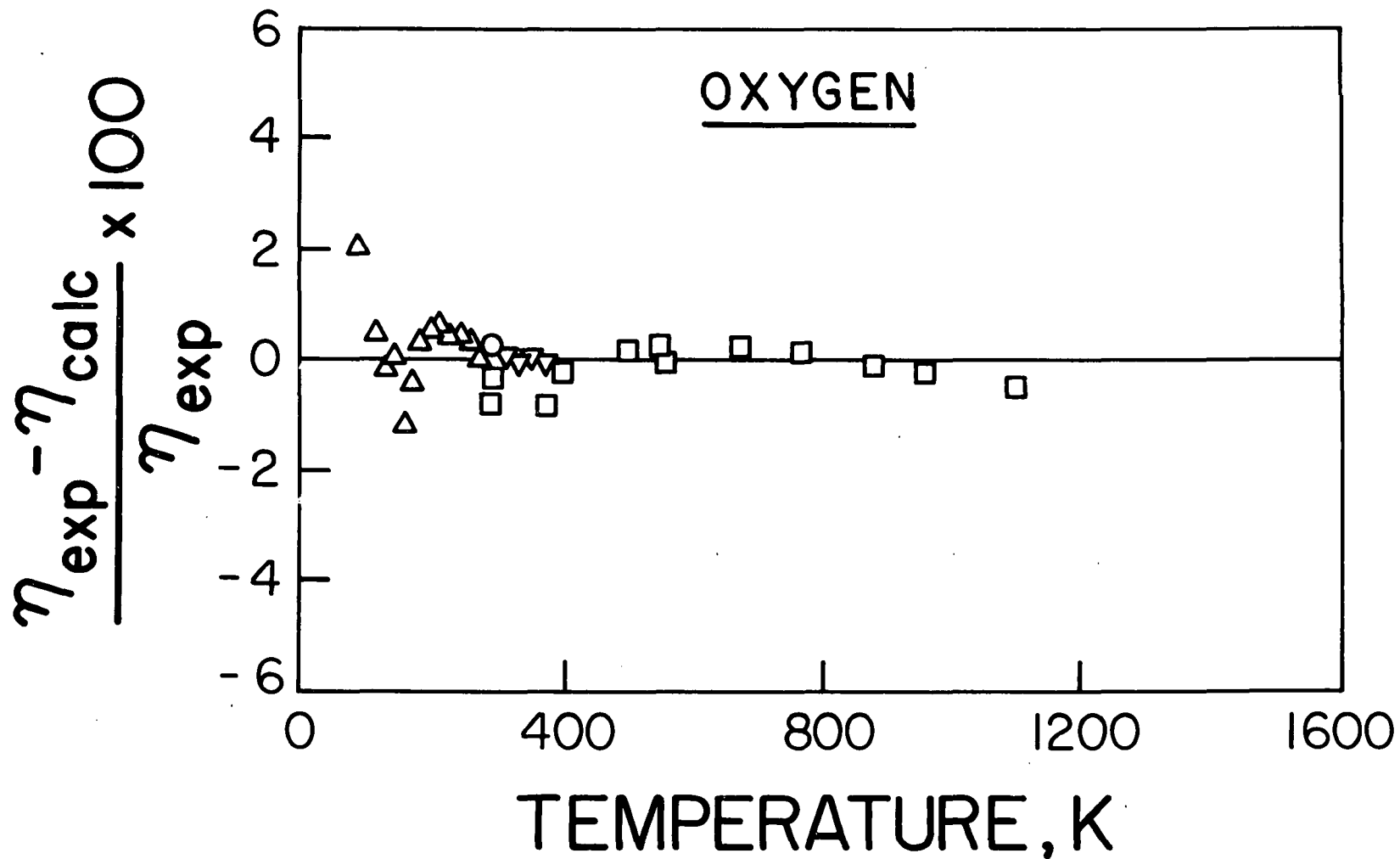
Figure 3. Difference between experimental and calculated viscosities of gaseous oxygen. Note that some of the experimental data have been adjusted as discussed in the text. Data: ∇[3], O[4], Δ[7, adjusted],☐[8,9, adjusted].
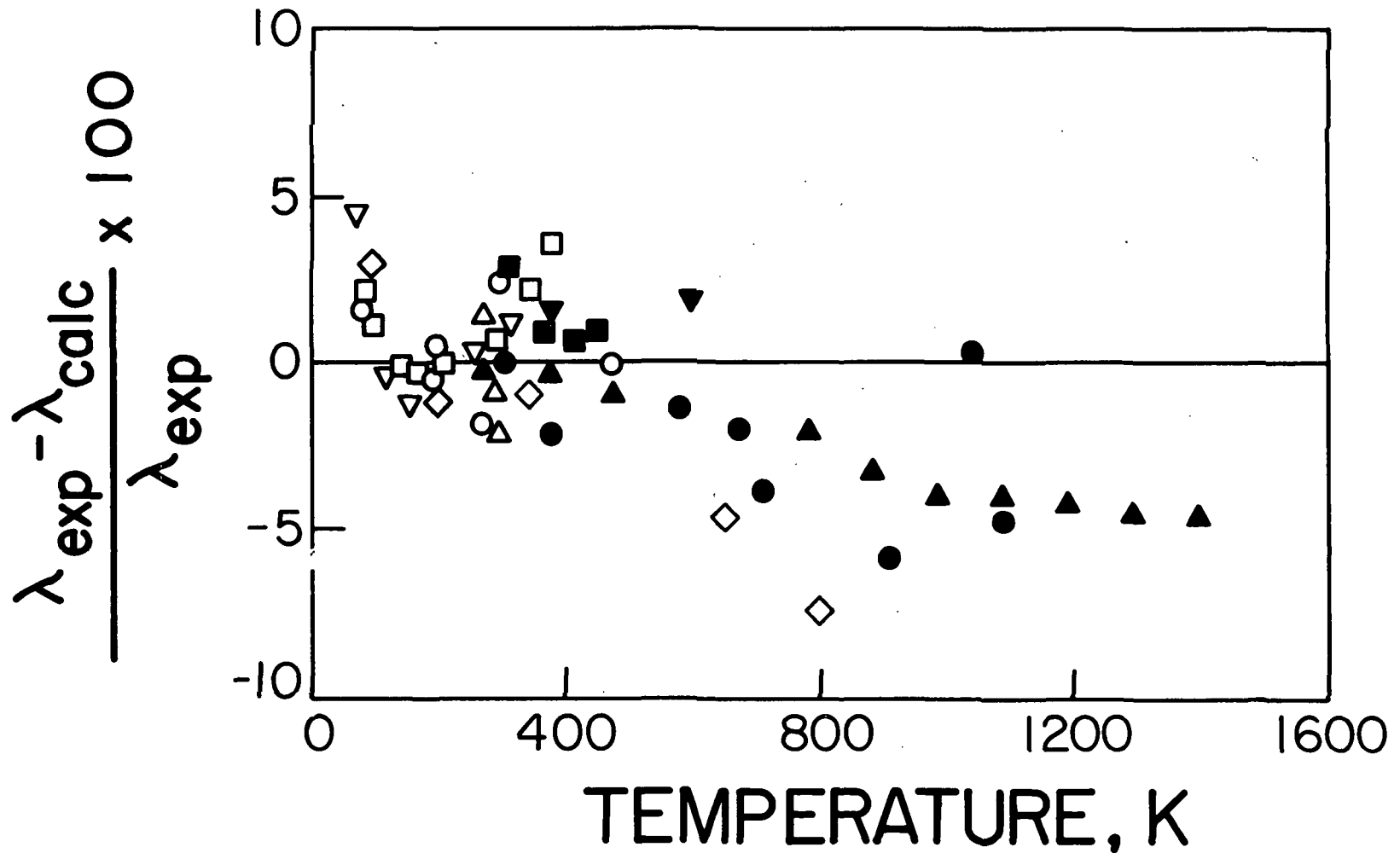
Figure 4. Difference between experimental and calculated thermal conductivities of gaseous oxygen. Data: O[17], ▲[18], ◇[19], △[20-22], □[23], ▽[24], ▼[25], ■[26], ●[27].

method to generate a table of values for $\eta_o(T)$ and $\lambda_o(T)$ (Table III in Section VI).

The uncertainty in the data and the approximations in the calculations make it difficult to assign an accuracy to the tabulated coefficients. On the basis of the deviation curves, however, we attribute an estimated uncertainty of 3% to the viscosity values at temperatures up to 1000 K, while the error could be as large as 5% at temperatures between 1000 K and 2000 K. The possible uncertainty in the thermal conductivity values is estimated to be 5% at all temperatures.

IV. Transport properties of the dense gas and liquid.

4.1 Excess functions

As a next step we need to estimate the excess functions $\Delta\eta(\rho)$ and $\Delta\lambda(\rho)$, introduced in equations (1), which account for the behavior of the transport coefficients of the dense gas and liquid at temperatures and densities away from the critical point. Many investigators have noted that these excess functions for fluids other than helium and hydrogen are nearly independent of temperature when plotted as a function of density [1,48]. Thus a considerable amount of data obtained at different densities and temperatures can be represented to a first approximation by a single curve as a function of density, including data for the saturated vapor and liquid. Conversely, use of the excess functions $\Delta\eta(\rho)$ and $\Delta\lambda(\rho)$ enables us to estimate values for the transport coefficients over a wide range of experimental conditions from experimental data in a narrow range of conditions.†

4.2 Application to oxygen.

The correlation technique used in this report is to fit selected experimental data with the assumption that *outside the critical region*

---

†The empirical rule that the excess functions are independent of the temperature is only approximately true. A small temperature dependence of the excess functions does exist which becomes more pronounced at large densities such as densities twice the critical densities. It turns out that at large densities $(\partial\Delta\eta/\partial T)_\rho$ is negative [1,48]. The rule breaks down for the thermal conductivity in the critical region where an additional anomalous contribution must be taken into account as discussed in Section V. In this latter case the more detailed equations (1a),(1b) have to be considered.

the excess functions $\Delta\eta(\rho)$ and $\Delta\lambda(\rho)$ are independent of the temperature.

The excess viscosity $\Delta\eta(\rho)$ was represented by the following two equations

For $\rho \leq 0.932$ g/cm^3

$$\Delta\eta(\rho) = 0.47293\rho - 0.17410\rho^2 + 0.59995\rho^3 \tag{11}$$

and for $\rho > 0.932$ g/cm^3

$$\Delta\eta(\rho) = 0.6539\rho + 0.000029886\exp(9.25\rho - 1.0)$$

where ρ is expressed in g/cm^3 and η in milligram/cm.s. These functions were chosen on the basis of the excess viscosity values deduced from the data of Grevendonk [30] and presented in Fig. 5. Data from ref. [4] and [31] were also used to check that in the limit of low densities $\Delta\eta(\rho)$ approached zero in a consistent manner. The excess viscosity was represented by the two equations in (11), because of the sharp increase of the slope at a density twice the critical density.

An equation for the excess thermal conductivity $\Delta\lambda(\rho)$ was obtained by fitting a polynomial to the excess values deduced from the experimental data of Ziebland and Burton [32].

$$\Delta\lambda(\rho) = 62.808\rho - 49.337\rho^2 + 252.43\rho^3 - 515.28\rho^4$$
$$+ 544.61\rho^5 - 189.91\rho^6 \tag{12}$$

where ρ is expressed in g/cm^3 and λ in milliwatt/m.K. The excess thermal conductivity is shown in Fig. 6.

I should be emphasized that equations (11) and (12) are *empirical*
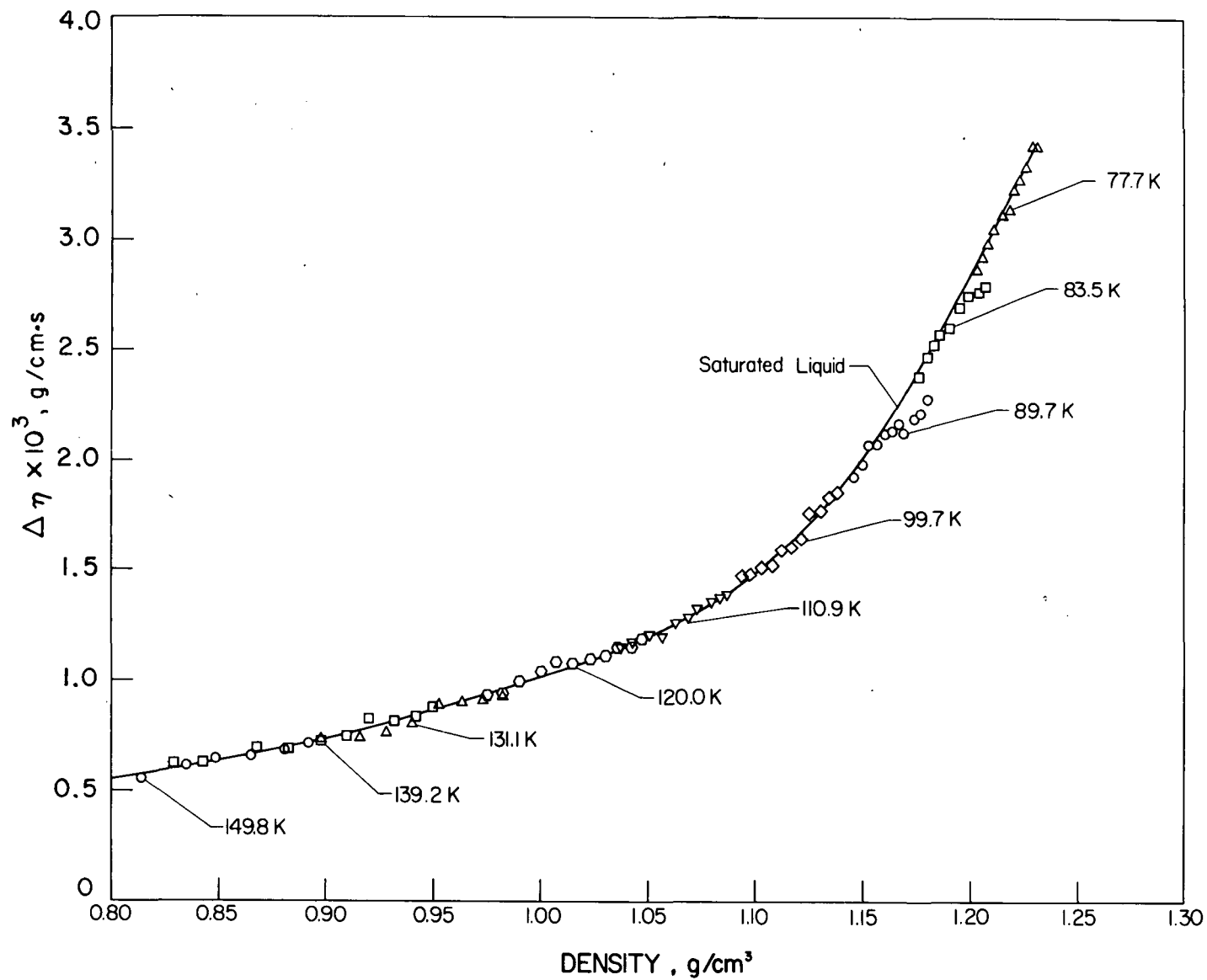
Figure 5. Excess viscosity $\Delta\eta(\rho)$ of oxygen as a function of density. The data were taken from ref. [30] and the curve represents equation (11).
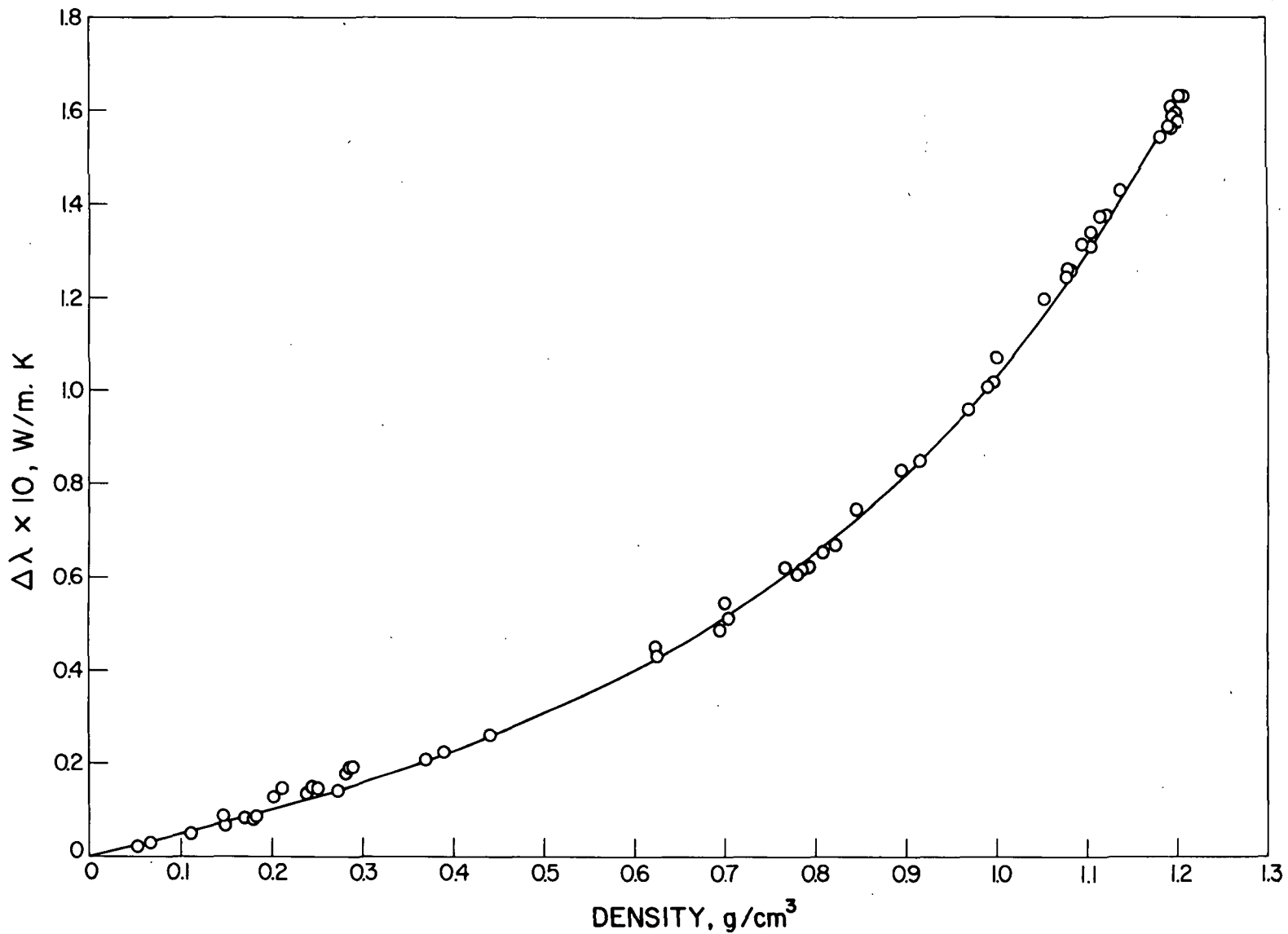
Figure 6.   Excess thermal conductivity $\Delta\lambda(\rho)$ of oxygen as a function of density.   The data were taken from ref. [32] and the curve represents equation (12).

representations for interpolating the experimental data. The kinetic

theory of gases predicts that the transport properties are nonanalytic

functions of the density and that the density expansions for viscosity

and thermal conductivity should contain terms such as $\rho^2 \ln\rho$. However,

the questions of how important such terms are in practice is presently

unresolved [49,50].

The excess values, $\Delta\eta(\rho)$ and $\Delta\lambda(\rho)$, calculated from equations (11)

and (12) were added to the dilute gas values, $\eta_o(T)$ and $\lambda_o(T)$, res-

pectively, obtained in Section III. The densities were converted into

pressures and vice versa using the equation of state. A discussion of

the equation of state of oxygen is beyond the scope of this report.

All calculations of the equilibrium properties in this report are

based on the equation of state developed by Stewart, Jacobsen and

Myers [51].

V. Thermal conductivity in the critical region.

5.1 Behavior of the transport properties near the critical point.

A survey of the behavior of the transport properties of fluids in the critical region was presented by one of us in a preceding technical report [2]. In order to account for this behavior we introduced in equations (1) anomalous contributions $\Delta_c \eta(\rho,T)$ and $\Delta_c \lambda(\rho,T)$ defined as

$$\Delta_c \eta(\rho,T) = \eta(\rho,T) - \eta_o(T) - \Delta\eta(\rho) \ , \tag{13a}$$

$$\Delta_c \lambda(\rho,T) = \lambda(\rho,T) - \lambda_o(T) - \Delta\lambda(\rho) \ , \tag{13b}$$

where $\Delta\eta(\rho)$ and $\Delta\lambda(\rho)$ are the temperature independent excess functions discussed in Section IV.

The viscosity appears to exhibit a weak anomaly and $\Delta_c \eta$ increases logarithmically as the critical point is approached [52]. However, the effect can only be noticed very close to the critical point and may be neglected for most engineering purposes [53]. The thermal conductivity, however, exhibits a strongly anomalous behavior which can be noticed in a large range of densities and temperatures around the critical point [53].

In a previous technical report we have argued that on approaching the critical point the asymptotic behavior of $\Delta_c \lambda(\rho,T)$ may be represented by

$$\Delta_c \lambda(\rho,T) = \frac{kT}{6\pi\eta\xi} \rho (c_p - c_v) \tag{14}$$

where c_p and c_v are the specific heats at constant pressure and volume and ξ is a length parameter known as the long range correlation length [2,54]. Equation (14) is based on the idea that the anomalous contribution to the thermal conductivity is determined by the mobility $kT/6\pi\eta\xi$ of clusters with an effective radius ξ. Using the thermodynamic relation

$$c_p - c_v = \frac{T}{\rho}\left(\frac{\partial P}{\partial T}\right)_\rho^2 K_T \tag{15}$$

where $K_T \equiv \rho^{-1}(\partial\rho/\partial P)_T$ is the isothermal compressibility, equation (14) can be rewritten as

$$\Delta_c\lambda(\rho,T) = \frac{kT^2}{6\pi\eta\xi}\left(\frac{\partial P}{\partial T}\right)_\rho^2 K_T \tag{16}$$

5.2 Equation for $\Delta_c\lambda(\rho,T)$

In order to discuss the critical enhancement in the thermal conductivity it is most convenient to consider the reduced variables

$$\Delta\tilde{T} = \frac{T - T_c}{T_c} \qquad\qquad \Delta\tilde{\rho} = \frac{\rho - \rho_c}{\rho_c} \tag{17}$$

where T_c, ρ_c are the temperature and density of the critical point. It should be emphasized that equations (14) and (16) represent the asymptotic behavior of $\Delta_c\lambda(\rho,T)$ in the limit $\Delta\tilde{T} \to 0$ and $\Delta\tilde{\rho} \to 0$. In practice, the validity of these equations is limited to the approximate range $|\Delta\tilde{T}| \lesssim 3\%$ and $|\Delta\tilde{\rho}| \lesssim 25\%$. However, experiments for carbon dioxide and steam indicate that the region of the actual anomalous behavior extends

as far as $|\Delta\tilde{T}| \simeq 20\%$ at $\rho = \rho_c$ and as far as $|\Delta\tilde{\rho}| \simeq 50\%$ at $T = T_c$ [55]. It is, therefore, necessary to develop a more general equation in order to represent the entire thermal conductivity anomaly.

A previous attempt to estimate the anomalous thermal conductivity $\Delta_c\lambda(\rho,T)$ was made by Hendricks and Baron [56]. Their approach was based on some theoretical considerations of Brokaw [57], but required the introduction of empirical adjustments. In this report we try to represent the anomalous thermal conductivity by a phenomenological equation which does reduce to the asymptotic behavior (16) in the limit $\Delta\tilde{T} \to 0$ and $\Delta\tilde{\rho} \to 0$ and vanishes for large values of $\Delta\tilde{T}$ and $\Delta\tilde{\rho}$. Specifically, we consider

$$\Delta_c\lambda(\rho,T) = \frac{kT^2}{6\pi\eta\xi}\left(\frac{\partial P}{\partial T}\right)_\rho^2 K_T \ \exp\{-\alpha|\Delta\tilde{T}|^2\}\exp\{-\beta|\Delta\tilde{\rho}|^4\} \qquad , \qquad (18)$$

The parameters α and β are related to the range of temperatures and pressures at which the anomalous thermal conductivity is observed. Experiment indicates that this range is the same for different gases [54]. The actual values for the parameters α and β were selected from an analysis of the observed thermal conductivity anomaly for CO_2[2], namely

$$\alpha = 18.66 \qquad , \qquad \beta = 4.25 \qquad . \qquad (19)$$

Equation (18) represents a preliminary empirical attempt to describe the anomalous thermal conductivity and will be subject to revision in the future. However, in Appendix B we provide evidence that equation (18) does approximate the observed anomalous thermal conductivity for a variety of fluids.

5.3 Correlation length

' Equation (18) contains the length ξ which is the range of the pair correlation function of the fluid. This range becomes very large near the critical point. The Ornstein-Zernike theory relates this long range correlation length to a short range correlation length R by the equation [58]

$$\xi = R\sqrt{nkTK_T} \qquad , \tag{20}$$

where n is the number density. The number density n in (20) is related to the mass density ρ by

$$n = \frac{N\rho}{M} \qquad , \tag{21}$$

where N is Avogadro's number and M the molar weight. In the approximation of the Ornstein-Zernike theory, ξ diverges as $\sqrt{K_T}$ when the critical point is approached, while R remains a finite parameter whose magnitude is of the order of the range of the intermolecular potential function. The long range correlation length ξ, and thus also the short range correlation length R, can be determined experimentally from light scattering or X-ray scattering data. Substitution of (20) and (21) into (18) yields

$$\Delta_c\lambda(\rho,T) = \left(\frac{M}{\rho NkT}\right)^{1/2} \frac{kT^2}{6\pi\eta R}\left(\frac{\partial P}{\partial T}\right)_\rho^2 \sqrt{K_T}\,\exp\{-\alpha|\tilde{\Delta T}|^2\}\exp\{-\beta|\tilde{\Delta\rho}|^4\} \quad . \tag{22}$$

In a previous technical report the parameter R was treated as a

constant independent of density and temperature [2]. However, as discussed in Appendix B, R appears more closely proportional to $\sqrt{n}$. Since at a given temperature $n^2 K_T$ is a function of ρ symmetric with respect to the critical density ρ_c [59,60], it follows from equation (20) that the assumption $R \propto \sqrt{n}$ is equivalent to the assumption that the correlation length ξ is symmetric around the critical density ρ_c.

Experimental data for the parameter R of fluids are scarce and imprecise, and nonexistent for oxygen. Therefore, we make an attempt to estimate R from the intermolecular potential function $\Phi(r)$. For this purpose we note that R^2 may be written as [58]

$$R^2 = \frac{n}{6} \int r^2 C(r) d\vec{r} \quad , \tag{23}$$

which is the second moment of the so-called short range correlation function $C(r)$. Under certain simplifying assumptions the behavior of $C(r)$ for large values of r, $(r \gg \sigma)$, may be approximated by $C(r) \simeq \Phi(r)/kT$ [61]. Accordingly we make the ansatz

$$R^2 = - \frac{n}{6kT} \int_{r_m}^{\infty} r^2 \Phi_{attr}(r) d\vec{r} \quad , \tag{24}$$

where $\Phi_{attr}(r)$ is the attractive part of the intermolecular potential function $\Phi(r)$ and r_m the distance corresponding to the potential minimum. Using the potential function (9), introduced in Section 3.3, we obtain

$$R = r_m \left(\frac{n^*}{T^*} \right)^{1/2} \left[\frac{2\pi}{3} \left\{ \frac{m - \gamma(m-8)}{m - 6} + \frac{\gamma}{3} \right\} \right]^{1/2} \quad , \tag{25}$$

where $T^* = kT/\varepsilon$ is the reduced temperature defined in (3) and n^*

is a reduced number density defined as

$$n^* = n r_m^3 \quad . \tag{26}$$

5.4 Application to oxygen

Our approach is to calculate $\Delta_c \lambda(\rho, T)$ from equation (22) with $\Delta \tilde{T}$ and

$\Delta \tilde{\rho}$ expressed in terms of the critical parameters of oxygen [51]

$$T_c = 154.581 \text{ K} \quad , \quad \rho_c = 0.4361 \text{ g/cm}^3 \quad . \tag{27}$$

The short range correlation length R is calculated from equation (25)

using the potential parameters (10) for oxygen.

Equation (22) relates the anomalous thermal conductivity $\Delta_c \lambda(\rho, T)$

to the calculated viscosities and the thermodynamic derivatives $(\partial P/\partial T)_\rho$

and K_T. These thermodynamic derivatives are to be obtained from the

equation of state.

The thermodynamic behavior of fluids near the critical point can

be described in terms of scaling laws [59,60,62]. Recently, we have

indeed formulated a scaled equation of state for oxygen, but further

• research is desirable before it can be used for extensive thermodynamic

calculations [63]. Moreover, the validity of the scaling law equation of

state is limited to the same range near the critical point, where the

asymptotic equation (14) applies. In order to calculate $\Delta_c \lambda(\rho, T)$ from (18) we

need an equation of state which not only covers the asymptotic range near

the critical point, but also connects this range with the P - ρ - T surface

further away from the critical point. Since such an equation of state is

28

not yet available, we have, for the purpose of this report, calculated

$(\partial P/\partial T)_{\rho}$ and K_T in (22) from the equation of state of Stewart, Jacobsen

and Myers [51]. This procedure has the advantage that all calculated

transport properties in this report are consistent with a single equation

of state and any discontinuities which might arise from the transition of

one equation of state to another are avoided. The procedure has the

disadvantage, however, that near the critical point the predicted thermal

conductivities are subject to errors because any analytic equation of

state, such as that of Stewart et al., will not yield accurate compress-

ibilities in the immediate vicinity of the critical point.[†]

The total excess thermal conductivity, defined as $\lambda(\rho,T) - \lambda_o(T) =$

$\Delta\lambda(\rho) + \Delta_c\lambda(\rho,T)$ is obtained by adding the contributions calculated from

equations (12) and (22). The behavior of the total excess thermal conduc-

tivity, thus calculated for oxygen in the critical region as a function

of density and temperature, is illustrated in Fig. 7.

It is difficult to estimate the reliability of the calculated thermal

conductivities in the vicinity of the critical point: it is influenced by

the use of the semi-empirical equation (22), by errors in the estimated

values for the parameter R and by errors in the compressibilities calculated

from the equation of state. An idea of the reliability of the procedure

may be obtained by investigating to what extent equation (22) represents

the thermal conductivities observed for other fluids, as discussed in

Appendix B. As a general rule the reliability of predicted thermal con-

[†] We plan to remedy this situation in our future research as discussed
in Section VII.
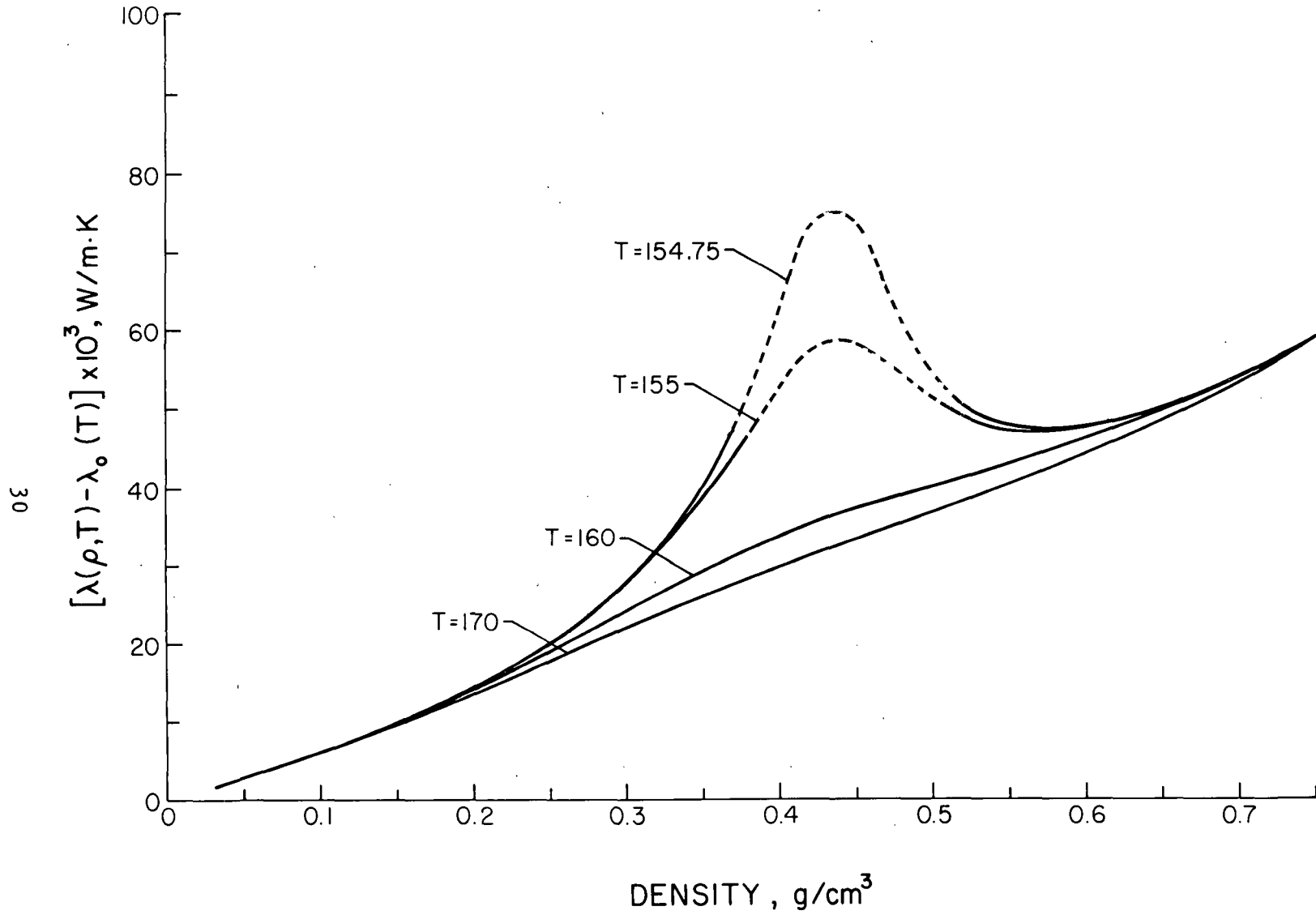
Figure 7. Total excess thermal conductivity, $\lambda(\rho, T) - \lambda_o(T)$, calculated for oxygen in the critical region.

ductivities in the vicinity of the critical point will always depend on how well one predicts the compressibility. For oxygen such an assessment can be made by comparing the equation of state of Stewart et al. [51] with a scaling law equation of state such as that obtained by Levelt Sengers, Greer and Sengers [63]. From such considerations we conclude that the errors may be larger than the overall estimated error of 15% in the region indicated by the dashed portions of the curves in Fig. 7.

VI. Results.

The values of the parameters used in the calculation of the

transport coefficients of oxygen are summarized in Table II.

The transport coefficients of gaseous oxygen at low pressures were

calculated at temperatures from 80 K to 2000 K by the method described in

Section III. The results are presented in Table III. The estimated

uncertainty of these values was also discussed in Section III and varies

from 2% to 5% depending on the property and temperature considered.

The values are presented to four decimals in order to facilitate inter-

polation. The shaded values at temperatures above 1000 K were obtained by

extrapolation from information available at temperatures below 1000K.

The transport coefficients of compressed oxygen were calculated at

temperatures from 80 K to 400 K and at pressures from 1 atm to 200 atm.

These values were obtained by adding to the dilute gas values the excess

functions as calculated form equations (11) and (12) and, for the thermal

conductivity, a critical enhancement calculated from equations (22) and

(25). The necessary equilibrium properties were calculated from the

equation of state in ref. [51].

The resulting values for the viscosity and thermal conductivity are

presented, respectively, in Tables IV and V as a function of temperature

and pressure. In view of the rapid variation of the thermal conductivity

in the critical region we have also generated Table VI which contains

the thermal conductivity at small intervals of temperature and pressure

32

in the region of interest. In Table VII we present the values calculated

for the transport coefficients of the saturated vapor and liquid. In all

tables[†] temperatures are expressed in K, pressures in international

atmospheres, viscosities in milligram/cm.s and thermal conductivities

in milliwatt/m.k. Conversion factors to other units are presented in

Table VIII for the benefit of the user.

The reliability of the calculated values is limited by a number of

factors, an important one being that only one source of data with uncertain

accuracy was available to determine the excess functions (11) and (12).

Near the critical point additional complications arise from the absence of

experimental data for the correlation length and the use of an analytic

equation of state as discussed earlier. Nevertheless, except for a region

in the vicinity of the critical point we estimate that the tabulated

values are reliable to within about 15%.

Previously estimated values for the transport coefficients of oxygen

are included in compilations prepared by the National Bureau of Standards

[64,65]. The values for the transport coefficients presented in this

report are based on a better and more systematic correlation procedure

for the viscosity and thermal conductivity of the dilute gas and for the

thermal conductivity anomaly in the critical region.

[†]   Computer programs that generate the tabulated values are obtainable,
    upon request, from the Cryogenic Data Center, National Bureau of
    Standards, Boulder, Colorado 80302.

Table II

Parameters for oxygen used in this report.

Potential parameters: (m - 6 - 8 potential). [40] $m = 10$, $\gamma = 1.0$, $\sigma = 3.437\overset{\circ}{A}$, $r_m = 3.8896\overset{\circ}{A}$, $\epsilon/k = 113.0$ K
Critical parameters [51] $T_c = 154.581$ K $\qquad \rho_c = 0.4361$ g/cm^3 $\qquad P_c = 49.77$ atm
Conversion factor from mass density ρ to number density n $\dfrac{N}{M} = 0.1882 \times 10^{-23}$ g^{-1}
Equation of state parameters: see ref. [51].

Table III

Viscosity $\eta_o(T)$ and thermal conductivity $\lambda_o(T)$ of gaseous oxygen as a function of temperature.

Temperature	Viscosity	Thermal Conductivity	Temperature	Viscosity	Thermal Conductivity
K	g/cm.s	W/m.K	K	g/cm.s	W/m.K
	$10^3\eta_o$	$10^3\lambda_o$		$10^3\eta_o$	$10^3\lambda_o$
80	0.0585	6.94	255	0.1810	22.89
85	0.0624	7.44	260	0.1840	23.29
90	0.0663	7.95	265	0.1869	23.69
95	0.0701	8.45	270	0.1898	24.08
100	0.0740	8.96	275	0.1927	24.47
			280	0.1955	24.86
105	0.0779	9.46	285	0.1984	25.24
110	0.0818	9.96	290	0.2012	25.62
115	0.0856	10.45	295	0.2040	26.00
120	0.0894	10.94	300	0.2068	26.38
125	0.0932	11.43			
130	0.0970	11.92	305	0.2095	26.76
135	0.1007	12.41	310	0.2122	27.14
140	0.1045	12.89	315	0.2150	27.52
145	0.1082	13.37	320	0.2176	27.89
150	0.1118	13.85	325	0.2203	28.25
			330	0.2230	28.62
155	0.1155	14.32	335	0.2256	28.99
160	0.1191	14.78	340	0.2282	29.36
165	0.1226	15.24	345	0.2308	29.76
170	0.1261	15.70	350	0.2334	30.10
175	0.1296	16.15			
180	0.1331	16.60	355	0.2359	30.48
185	0.1365	17.04	360	0.2385	30.85
190	0.1399	17.48	365	0.2410	31.22
195	0.1432	17.92	370	0.2435	31.58
200	0.1465	18.35	375	0.2460	31.95
			380	0.2485	32.32
205	0.1498	18.78	385	0.2510	32.69
210	0.1530	19.21	390	0.2534	33.06
215	0.1563	19.63	395	0.2559	33.42
220	0.1595	20.05	400	0.2583	33.79
225	0.1626	20.47			
230	0.1658	20.88	405	0.2607	34.16
235	0.1689	21.28	410	0.2631	34.54
240	0.1719	21.69	415	0.2655	34.91
245	0.1750	22.09	420	0.2678	35.28
250	0.1780	22.49	425	0.2702	35.65

Table III (continued)

Temperature K	Viscosity g/cm.s $10^3\eta_o$	Thermal Conductivity W/m.K $10^3\lambda_o$	Temperature K	Viscosity g/cm.s $10^3\eta_o$	Thermal Conductivity W/m.K $10^3\lambda_o$
430	0.2725	36.02	810	0.4255	62.51
435	0.2748	36.38	820	0.4290	63.16
440	0.2772	36.75	830	0.4326	63.81
445	0.2795	37.12	840	0.4361	64.45
450	0.2818	37.49	850	0.4396	65.09
			860	0.4430	65.71
455	0.2840	37.85	870	0.4466	66.35
460	0.2863	38.22	880	0.4500	66.98
465	0.2886	38.59	890	0.4535	67.61
470	0.2908	38.95	900	0.4569	68.23
475	0.2931	39.32			
480	0.2953	39.68	910	0.4603	68.89
485	0.2975	40.05	920	0.4637	69.50
490	0.2997	40.41	930	0.4671	70.11
495	0.3019	40.77	940	0.4705	70.72
500	0.3041	41.14	950	0.4738	71.33
			960	0.4772	71.93
510	0.3085	41.86	970	0.4805	72.52
520	0.3128	42.58	980	0.4838	73.12
530	0.3170	43.29	990	0.4872	73.73
540	0.3213	44.01	1000	0.4905	74.32
550	0.3255	44.72			
560	0.3297	45.44	1010	0.4937	74.91
570	0.3338	46.14	1020	0.4970	75.49
580	0.3379	46.86	1030	0.5002	76.07
590	0.3420	47.56	1040	0.5035	76.66
600	0.3460	48.27	1050	0.5068	77.26
			1060	0.5100	77.84
610	0.3501	48.97	1070	0.5132	78.42
620	0.3541	49.68	1080	0.5164	78.99
630	0.3580	50.37	1090	0.5196	79.56
640	0.3619	51.08	1100	0.5228	80.14
650	0.3659	51.77			
660	0.3697	52.46	1110	0.5259	80.71
670	0.3736	53.16	1120	0.5291	81.27
680	0.3774	53.85	1130	0.5322	81.84
690	0.3813	54.54	1140	0.5353	82.40
700	0.3851	55.22	1150	0.5384	82.97
			1160	0.5416	83.54
710	0.3888	55.89	1170	0.5447	84.10
720	0.3926	56.57	1180	0.5478	84.66
730	0.3963	57.25	1190	0.5509	85.21
740	0.4000	57.92	1200	0.5540	85.77
750	0.4037	58.59			
760	0.4074	59.24	1210	0.5571	86.32
770	0.4110	59.90	1220	0.5601	86.87
780	0.4147	60.57	1230	0.5632	87.42
790	0.4183	61.22	1240	0.5662	87.97
800	0.4218	61.87	1250	0.5692	88.51

Table III (continued)

Temperature	Viscosity	Thermal Conductivity	Temperature	Viscosity	Thermal Conductivity
K	g/cm.s $10^3\eta_o$	W/m.K $10^3\lambda_o$	K	g/cm.s $10^3\eta_o$	W/m.K $10^3\lambda_o$
1260	0.5722	89.06	1660	0.6871	110.05
1270	0.5753	89.61	1670	0.6899	110.56
1280	0.5783	90.16	1680	0.6926	111.07
1290	0.5813	90.70	1690	0.6953	111.58
1300	0.5843	91.24	1700	0.6980	112.08
1310	0.5873	91.78	1710	0.7007	112.58
1320	0.5903	92.32	1720	0.7034	113.09
1330	0.5932	92.85	1730	0.7062	113.60
1340	0.5962	93.39	1740	0.7089	114.11
1350	0.5991	93.92	1750	0.7116	114.61
1360	0.6021	94.45	1760	0.7143	115.11
1370	0.6050	94.99	1770	0.7169	115.62
1380	0.6079	95.52	1780	0.7196	116.12
1390	0.6109	96.06	1790	0.7223	116.63
1400	0.6138	96.59	1800	0.7250	117.13
1410	0.6167	97.11	1810	0.7276	117.63
1420	0.6196	97.64	1820	0.7303	118.13
1430	0.6225	98.17	1830	0.7329	118.63
1440	0.6254	98.69	1840	0.7355	119.12
1450	0.6282	99.22	1850	0.7382	119.63
1460	0.6311	99.74	1860	0.7409	120.13
1470	0.6340	100.27	1870	0.7435	120.63
1480	0.6368	100.78	1880	0.7461	121.13
1490	0.6396	101.30	1890	0.7487	121.63
1500	0.6425	101.83	1900	0.7514	122.13
1510	0.6454	102.35	1910	0.7548	122.63
1520	0.6482	102.86	1920	0.7566	123.13
1530	0.6510	103.38	1930	0.7592	123.62
1540	0.6538	103.90	1940	0.7618	124.11
1550	0.6566	104.41	1950	0.7643	124.61
1560	0.6594	104.93	1960	0.7670	125.11
1570	0.6622	105.45	1970	0.7696	125.61
1580	0.6650	105.96	1980	0.7721	126.11
1590	0.6678	106.47	1990	0.7747	126.60
1600	0.6706	106.98	2000	0.7773	127.10
1610	0.6733	107.49			
1620	0.6761	108.01			
1630	0.6789	108.52			
1640	0.6816	109.03			
1650	0.6844	109.54			

Note: Shaded data are extrapolated data.

Table IV

Viscosity of compressed oxygen (η in milligram/cm,s)

T,K \ P,atm	1	5	10	15	20	25	30	35	40	45	50	55
80	2.648	2.661	2.677	2.693	2.708	2.724	2.740	2.756	2.772	2.788	2.804	2.820
90	1.969	1.979	1.992	2.005	2.018	2.031	2.044	2.057	2.070	2.083	2.096	2.109
100	0.076	1.512	1.523	1.533	1.544	1.554	1.565	1.576	1.586	1.597	1.608	1.619
110	0.083	0.091	1.198	1.207	1.216	1.225	1.234	1.243	1.252	1.261	1.270	1.279
120	0.091	0.098	0.108	0.979	0.987	0.995	1.003	1.011	1.019	1.026	1.034	1.042
130	0.098	0.105	0.113	0.123	0.827	0.834	0.841	0.847	0.854	0.860	0.866	0.872
140	0.106	0.111	0.119	0.127	0.137	0.150	0.702	0.714	0.725	0.734	0.744	0.752
150	0.113	0.118	0.125	0.133	0.141	0.150	0.162	0.176	0.199	0.561	0.586	0.605
160	0.120	0.125	0.131	0.138	0.145	0.153	0.162	0.172	0.184	0.198	0.218	0.251
170	0.127	0.132	0.137	0.144	0.150	0.157	0.164	0.172	0.181	0.191	0.203	0.216
180	0.134	0.138	0.144	0.149	0.155	0.161	0.168	0.175	0.182	0.190	0.199	0.208
190	0.141	0.145	0.150	0.155	0.161	0.166	0.172	0.178	0.185	0.191	0.198	0.206
200	0.147	0.151	0.156	0.161	0.166	0.171	0.176	0.182	0.188	0.194	0.200	0.206
210	0.154	0.157	0.162	0.167	0.171	0.176	0.181	0.186	0.191	0.197	0.202	0.208
220	0.160	0.164	0.168	0.172	0.177	0.181	0.186	0.191	0.195	0.200	0.205	0.211
230	0.167	0.170	0.174	0.178	0.182	0.187	0.191	0.195	0.200	0.204	0.209	0.214
240	0.173	0.176	0.180	0.184	0.188	0.192	0.196	0.200	0.204	0.208	0.213	0.217
250	0.179	0.182	0.185	0.189	0.193	0.197	0.201	0.205	0.209	0.213	0.217	0.221
260	0.185	0.188	0.191	0.195	0.198	0.202	0.206	0.209	0.213	0.217	0.221	0.225
270	0.190	0.193	0.197	0.200	0.204	0.207	0.211	0.214	0.218	0.221	0.225	0.229
280	0.196	0.199	0.202	0.205	0.209	0.212	0.216	0.219	0.222	0.226	0.229	0.233
290	0.202	0.204	0.208	0.211	0.214	0.217	0.220	0.224	0.227	0.230	0.233	0.237
300	0.207	0.210	0.213	0.216	0.219	0.222	0.225	0.228	0.232	0.235	0.238	0.241
310	0.213	0.215	0.218	0.221	0.224	0.227	0.230	0.233	0.236	0.239	0.242	0.245
320	0.218	0.221	0.223	0.226	0.229	0.232	0.235	0.238	0.241	0.244	0.246	0.249
330	0.224	0.226	0.229	0.231	0.234	0.237	0.240	0.242	0.245	0.248	0.251	0.254
340	0.229	0.231	0.234	0.236	0.239	0.242	0.244	0.247	0.250	0.252	0.255	0.258
350	0.234	0.236	0.239	0.241	0.244	0.247	0.249	0.252	0.254	0.257	0.260	0.262
360	0.239	0.241	0.244	0.246	0.249	0.251	0.254	0.256	0.259	0.261	0.264	0.266
370	0.244	0.246	0.249	0.251	0.253	0.256	0.258	0.261	0.263	0.266	0.268	0.271
380	0.249	0.251	0.253	0.256	0.258	0.261	0.263	0.265	0.268	0.270	0.272	0.275
390	0.254	0.256	0.258	0.260	0.263	0.265	0.267	0.270	0.272	0.274	0.277	0.279
400	0.259	0.261	0.263	0.265	0.267	0.270	0.272	0.274	0.277	0.279	0.281	0.283

Table IV (continued)

Viscosity of compressed oxygen (η in milligram/cm.s)

T,K \ P,atm	60	65	70	80	90	100	110	120	130	150	175	200
80	2.836	2.853	2.869	2.901	2.934	2.967	3.000	3.033	3.067	3.134	3.219	3.305
90	2.122	2.135	2.148	2.175	2.201	2.228	2.255	2.282	2.309	2.363	2.432	2.502
100	1.629	1.640	1.651	1.673	1.694	1.716	1.738	1.760	1.782	1.827	1.883	1.940
110	1.288	1.297	1.306	1.325	1.343	1.361	1.379	1.397	1.415	1.452	1.498	1.545
120	1.050	1.058	1.066	1.081	1.097	1.112	1.127	1.143	1.158	1.189	1.228	1.267
130	0.879	0.886	0.893	0.907	0.921	0.935	0.949	0.962	0.976	1.002	1.036	1.069
140	0.761	0.769	0.776	0.790	0.804	0.816	0.828	0.839	0.850	0.870	0.897	0.926
150	0.628	0.636	0.649	0.672	0.691	0.709	0.725	0.739	0.753	0.778	0.806	0.831
160	0.331	0.423	0.472	0.527	0.564	0.592	0.616	0.636	0.655	0.687	0.721	0.751
170	0.232	0.251	0.277	0.346	0.412	0.462	0.500	0.530	0.555	0.597	0.638	0.673
180	0.218	0.230	0.242	0.273	0.311	0.353	0.394	0.430	0.461	0.512	0.561	0.601
190	0.214	0.223	0.232	0.252	0.275	0.302	0.331	0.360	0.389	0.440	0.493	0.537
200	0.213	0.220	0.228	0.243	0.261	0.280	0.300	0.322	0.344	0.389	0.439	0.483
210	0.214	0.220	0.226	0.240	0.254	0.269	0.285	0.302	0.319	0.355	0.400	0.441
220	0.216	0.221	0.227	0.238	0.250	0.263	0.276	0.290	0.305	0.334	0.372	0.409
230	0.218	0.223	0.228	0.239	0.249	0.260	0.272	0.284	0.296	0.321	0.354	0.386
240	0.222	0.226	0.231	0.240	0.250	0.259	0.270	0.280	0.291	0.313	0.341	0.370
250	0.225	0.229	0.233	0.242	0.251	0.260	0.269	0.278	0.288	0.307	0.332	0.358
260	0.228	0.232	0.236	0.244	0.252	0.261	0.269	0.278	0.286	0.304	0.327	0.350
270	0.232	0.236	0.240	0.247	0.255	0.262	0.270	0.278	0.286	0.302	0.323	0.344
280	0.236	0.240	0.243	0.250	0.257	0.264	0.272	0.279	0.286	0.301	0.321	0.340
290	0.240	0.243	0.247	0.253	0.260	0.267	0.274	0.281	0.288	0.302	0.319	0.337
300	0.244	0.247	0.250	0.257	0.263	0.270	0.276	0.283	0.289	0.302	0.319	0.335
310	0.248	0.251	0.254	0.260	0.266	0.272	0.279	0.285	0.291	0.303	0.319	0.335
320	0.252	0.255	0.258	0.264	0.270	0.275	0.281	0.287	0.293	0.305	0.320	0.334
330	0.256	0.259	0.262	0.268	0.273	0.279	0.284	0.290	0.295	0.307	0.321	0.335
340	0.261	0.263	0.266	0.271	0.277	0.282	0.287	0.293	0.298	0.309	0.322	0.336
350	0.265	0.267	0.270	0.275	0.280	0.285	0.291	0.296	0.301	0.311	0.324	0.337
360	0.269	0.271	0.274	0.279	0.284	0.289	0.294	0.299	0.304	0.314	0.326	0.338
370	0.273	0.275	0.278	0.283	0.288	0.292	0.297	0.302	0.307	0.316	0.328	0.340
380	0.277	0.280	0.282	0.287	0.291	0.296	0.300	0.305	0.310	0.319	0.330	0.342
390	0.281	0.284	0.286	0.290	0.295	0.299	0.304	0.308	0.313	0.322	0.333	0.344
400	0.285	0.288	0.290	0.294	0.299	0.303	0.307	0.312	0.316	0.325	0.335	0.346

Table V

Thermal conductivity of compressed oxygen (λ in milliwatt/m,K)

T,K \ P,atm	1	5	10	15	20	25	30	35	40	45	50	55
80	164.7	164.9	165.2	165.4	165.7	165.9	166.2	166.4	166.7	166.9	167.1	167.4
90	151.8	152.0	152.3	152.6	152.9	153.3	153.6	153.9	154.2	154.5	154.8	155.1
100	9.5	138.4	138.8	139.2	139.6	140.0	140.4	140.8	141.1	141.5	141.9	142.3
110	10.4	11.4	124.9	125.3	125.8	126.3	126.8	127.3	127.7	128.2	128.6	129.1
120	11.4	12.2	13.5	110.9	111.5	112.1	112.8	113.3	113.9	114.5	115.1	115.6
130	12.3	13.1	14.2	15.6	96.3	97.1	98.0	98.8	99.6	100.3	101.1	101.8
140	13.2	14.0	15.0	16.1	17.5	19.3	81.6	82.9	84.1	85.2	86.3	87.3
150	14.1	14.8	15.7	16.7	17.9	19.2	20.9	23.3	27.8	68.4	70.4	72.1
160	15.8	15.7	16.5	17.4	18.4	19.5	20.7	22.3	24.2	26.7	30.5	37.3
170	15.9	16.5	17.3	18.1	19.0	19.9	20.9	22.1	23.4	24.9	26.8	29.0
180	16.8	17.4	18.1	18.8	19.6	20.4	21.3	22.3	23.3	24.4	25.7	27.1
190	17.7	18.2	18.9	19.5	20.3	21.0	21.8	22.6	23.5	24.4	25.4	26.4
200	18.5	19.0	19.6	20.3	20.9	21.6	22.3	23.0	23.8	24.6	25.4	26.3
210	19.3	19.8	20.4	21.0	21.6	22.3	22.9	23.6	24.2	24.9	25.7	26.4
220	20.2	20.6	21.2	21.7	22.3	22.9	23.5	24.1	24.7	25.4	26.0	26.7
230	21.0	21.4	21.9	22.5	23.0	23.6	24.1	24.7	25.3	25.9	26.5	27.1
240	21.7	22.2	22.7	23.2	23.7	24.2	24.8	25.3	25.8	26.4	26.9	27.5
250	22.5	22.9	23.4	23.9	24.4	24.9	25.4	25.9	26.4	26.9	27.5	28.0
260	23.3	23.7	24.1	24.6	25.1	25.6	26.0	26.5	27.0	27.5	28.0	28.5
270	24.0	24.4	24.9	25.3	25.8	26.2	26.7	27.1	27.6	28.1	28.5	29.0
280	24.8	25.1	25.6	26.0	26.4	26.9	27.3	27.8	28.2	28.6	29.1	29.5
290	25.5	25.9	26.3	26.7	27.1	27.5	28.0	28.4	28.8	29.2	29.6	30.1
300	26.2	26.6	27.0	27.4	27.8	28.2	28.6	29.0	29.4	29.8	30.2	30.6
310	27.0	27.3	27.7	28.1	28.5	28.8	29.2	29.6	30.0	30.4	30.8	31.2
320	27.7	28.0	28.4	28.7	29.1	29.5	29.9	30.2	30.6	31.0	31.4	31.7
330	28.4	28.7	29.0	29.4	29.8	30.1	30.5	30.9	31.2	31.6	31.9	32.3
340	29.1	29.3	29.7	30.1	30.4	30.8	31.1	31.5	31.8	32.2	32.5	32.9
350	29.7	30.0	30.4	30.7	31.1	31.4	31.7	32.1	32.4	32.8	33.1	33.4
360	30.4	30.7	31.0	31.4	31.7	32.0	32.4	32.7	33.0	33.3	33.7	34.0
370	31.1	31.4	31.7	32.0	32.3	32.7	33.0	33.3	33.6	33.9	34.3	34.6
380	31.8	32.0	32.3	32.7	33.0	33.3	33.6	33.9	34.2	34.5	34.8	35.1
390	32.4	32.7	33.0	33.3	33.6	33.9	34.2	34.5	34.8	35.1	35.4	35.7
400	33.1	33.3	33.6	33.9	34.2	34.5	34.8	35.1	35.4	35.7	36.0	36.3

Table V (continued)

Thermal conductivity of compressed oxygen (λ in milliwatt/m.K)

P, atm T, K	60	65	70	80	90	100	110	120	130	150	175	200
80	167.6	167.9	168.1	168.6	169.1	169.5	170.0	170.4	170.9	171.8	172.8	173.9
90	155.4	155.7	156.0	156.6	157.1	157.7	158.3	158.8	159.4	160.4	161.8	163.0
100	142.6	143.0	143.3	144.0	144.7	145.4	146.1	146.8	147.4	148.7	150.3	151.8
110	129.5	130.0	130.4	131.2	132.1	132.9	133.7	134.5	135.3	136.8	138.6	140.4
120	116.2	115.7	117.2	118.3	119.3	120.3	121.2	122.2	123.1	124.9	127.0	129.0
130	102.5	103.2	103.9	105.2	106.4	107.6	108.8	109.9	111.0	113.1	115.6	117.9
140	88.3	89.2	90.1	91.8	93.4	95.0	96.4	97.8	99.1	101.6	104.5	107.1
150	73.5	74.9	76.2	78.5	80.5	82.5	84.2	85.9	87.5	90.5	93.8	96.9
160	50.2	57.8	61.3	65.6	68.6	71.0	73.1	75.1	76.9	80.2	83.9	87.3
170	31.7	35.1	39.2	47.9	54.7	59.3	62.7	65.3	67.6	71.3	75.3	78.9
180	28.7	30.4	32.4	36.9	42.0	47.0	51.3	55.0	58.1	63.0	67.7	71.5
190	27.6	28.8	30.1	33.0	36.2	39.6	43.2	46.5	49.7	55.1	60.5	64.8
200	27.2	28.1	29.1	31.3	33.6	36.1	38.7	41.4	44.0	48.9	54.3	58.9
210	27.2	28.0	28.8	30.5	32.4	34.4	36.4	38.5	40.6	44.9	49.8	54.1
220	27.4	28.1	28.8	30.3	31.9	33.5	35.2	36.9	38.7	42.3	46.6	50.7
230	27.7	28.3	29.0	30.3	31.7	33.1	34.6	36.1	37.6	40.7	44.5	48.2
240	28.1	28.7	29.2	30.5	31.7	33.0	34.3	35.6	36.9	39.7	43.1	46.4
250	28.5	29.1	29.6	30.7	31.8	33.0	34.2	35.4	36.6	39.0	42.1	45.2
260	29.0	29.5	30.0	31.0	32.1	33.1	34.2	35.3	36.4	38.7	41.5	44.2
270	29.5	29.9	30.4	31.4	32.4	33.3	34.4	35.4	36.4	38.4	41.0	43.6
280	30.0	30.4	30.9	31.8	32.7	33.6	34.6	35.5	36.5	38.4	40.8	43.2
290	30.5	30.9	31.3	32.2	33.1	33.9	34.8	35.7	36.6	38.4	40.6	42.9
300	31.0	31.4	31.8	32.7	33.5	34.3	35.1	36.0	36.8	38.5	40.6	42.7
310	31.6	31.9	32.3	33.1	33.9	34.7	35.5	36.3	37.1	38.7	40.6	42.6
320	32.1	32.5	32.8	33.6	34.3	35.1	35.8	36.6	37.4	38.9	40.8	42.6
330	32.8	33.0	33.4	34.1	34.8	35.5	36.2	37.0	37.7	39.1	40.9	42.7
340	33.2	33.5	33.9	34.6	35.3	36.0	36.7	37.3	38.0	39.4	41.1	42.8
350	33.8	34.1	34.4	35.1	35.8	36.4	37.1	37.7	38.4	39.7	41.4	43.0
360	34.3	34.6	35.0	35.6	36.2	36.9	37.5	38.2	38.8	40.1	41.7	43.2
370	34.9	35.2	35.5	36.1	36.7	37.4	38.0	38.6	39.2	40.4	42.0	43.5
380	35.4	35.7	36.0	36.6	37.2	37.8	38.4	39.0	39.6	40.8	42.3	43.7
390	36.0	36.3	36.6	37.2	37.8	38.3	38.9	39.5	40.1	41.2	42.6	44.0
400	36.6	36.9	37.1	37.7	38.3	38.8	39.4	40.0	40.5	41.6	43.0	44.3

Table VI

Thermal conductivity of oxygen in the critical region (λ in milliwatt/m.K)

P, atm T,K	35	40	45	48	50	52	55	60	65	70	80	90
135	91.1	92.0	93.0	93.5	93.8	94.2	94.7	95.5	96.3	97.1	98.5	100.0
140	82.9	84.1	85.2	85.9	86.3	86.7	87.3	88.3	89.2	90.1	91.8	93.4
145	74.0	75.7	77.2	78.0	78.5	79.0	79.8	81.0	82.1	83.1	85.1	86.9
150	23.3	27.8	68.4	69.6	70.4	71.1	72.1	73.5	74.9	76.2	78.5	80.5
151	23.1	26.9	66.4	67.8	68.6	69.4	70.5	72.1	73.5	74.8	77.2	79.3
152	22.9	26.3	36.1	65.8	66.8	67.6	68.8	70.5	72.1	73.4	75.9	78.1
153	22.8	25.8	32.4	63.7	64.7	65.8	67.1	69.0	70.6	72.1	74.6	76.8
154	22.7	25.5	30.6	40.0	62.6	63.7	65.3	67.4	69.2	70.7	73.3	75.6
155	22.6	25.1	29.4	34.7	46.4	61.6	63.2	65.7	67.7	69.3	72.1	74.4
156	22.5	24.9	28.6	32.5	37.3	51.8	60.8	63.9	66.1	67.9	70.8	73.3
157	22.4	24.7	28.0	31.1	34.3	39.9	56.9	61.7	64.4	66.4	69.5	72.1
158	22.4	24.5	27.5	30.1	32.6	36.2	46.6	59.2	62.5	64.9	68.3	70.9
159	22.3	24.3	27.1	29.4	31.4	34.1	40.5	55.4	60.4	63.2	66.9	69.7
160	22.3	24.2	26.7	28.8	30.5	32.7	37.3	50.2	57.8	61.3	65.6	68.6
165	22.1	23.7	25.6	26.9	28.0	29.2	31.2	35.8	42.0	48.7	57.5	62.2
170	22.1	23.4	24.9	26.0	26.8	27.6	29.0	31.7	35.1	39.2	47.9	54.7
175	22.2	23.3	24.6	25.5	26.1	26.7	27.8	29.8	32.1	34.7	41.0	47.3
180	22.3	23.3	24.4	25.2	25.7	26.2	27.1	28.7	30.4	32.4	36.9	42.0
185	22.4	23.4	24.4	25.0	25.5	25.9	26.7	28.0	29.4	31.0	34.5	38.5
190	22.6	23.5	24.4	25.0	25.4	25.8	26.4	27.6	28.8	30.1	33.0	36.2

Table VII

Transport Coefficients of Oxygen at Saturation

Temperature	Pressure	Viscosity		Thermal Conductivity	
K	atm	vap.	liq.	vap.	liq.
		milligram/cm.s		milliwatt/m.K	
80	0.30	0.059	2.652	7.4	164.7
90	0.98	0.068	1.971	8.5	151.8
100	2.51	0.079	1.504	9.9	138.2
110	5.36	0.092	1.188	11.5	124.3
120	10.09	0.108	0.971	13.6	110.3
130	17.26	0.129	0.824	16.3	95.9
140	27.52	0.158	0.696	20.1	80.6
142	30.00	0.166	0.668	21.1	77.4
144	32.64	0.175	0.638	22.3	74.0
146	35.45	0.185	0.607	23.6	70.6
148	38.44	0.197	0.574	25.2	67.0
150	41.61	0.211	0.537	27.2	63.2
152	45.00	0.231	0.494	29.9	58.7
154	48.65	0.269	0.424	35.2	52.0

Table VIII

Conversion factors

$T, K \longrightarrow T, °F$: multiply by (9/5) then subtract 459.67

$T, K \longrightarrow T, °C$: subtract 273.15

$T, K \longrightarrow T, °R$: multiply by (9/5)

$P, atm \longrightarrow P, psia$: multiply by 14.69595

$P, atm \longrightarrow P, N/m^2$: multiply by 1.01325×10^5

$\eta, g/cm.s \longrightarrow \eta, Ns/m^2$: multiply by 10^{-1}

$\eta, g/cm.s \longrightarrow \eta, lb_m/ft.s$: multiply by 0.0671969

$\lambda, W/m.K \longrightarrow \lambda, cal/cm.s.K$: multiply by (1/418.4)

$\lambda, W/m.K \longrightarrow \lambda, BTU/ft.hr.°R$: multiply by 0.578176

VII. Remarks.

With the exception of the immediate vicinity of the critical point,

the tables of transport coefficients presented in this report should be

adequate for those engineering applications where a 15% accuracy is

sufficient. In this section we mention some research items that need to

be considered in order to improve the accuracy of tabulated values for the

transport coefficients of oxygen. However, it should be emphasized

that the tabulation is severely hampered by the lack of reliable data

for oxygen. Until this situation is rectified, tables of transport

coefficients must be considered to be of a provisional nature.[†]

The present tabulation is based on the following approximations:

a. The dilute gas properties were calculated using a spherically

symmetric approximation to the intermolecular potential function.

For a more accurate representation of the dilute gas properties

of oxygen one should consider an angular dependent potential

function.

b. The excess functions (11) and (12) were determined from a very

limited set of data and were assumed to be independent of

temperature. However, the excess functions are known to have a

small temperature dependence which should be taken into account

for a more accurate tabulation.

c. The critical enhancement in the thermal conductivity was

calculated from a semi-theoretical equation which, at this time,

---

[†] Dr. W. M. Haynes of the Cryogenics Division of the National Bureau of
Standards is currently measuring the viscosity of oxygen over a wide
range of temperatures and pressures.

cannot be tested against any experimental data for oxygen. Moreover, the critical enhancement in the thermal conductivity is related to the square root of the compressibility which was calculated from an analytic equation of state. For a more accurate representation near the critical point the compressibility should be deduced from an equation of state that satisfies the scaling laws [63].

Work is in progress at the National Bureau of Standards and at the University of Maryland to improve upon these approximations. In the mean time we recommend use of the values presented in this report.

Appendix A

Dilute gas properties of oxygen

A.1 Introduction.

In Section III we calculated the viscosity and thermal conductivity

of gaseous oxygen using the potential function (9) with parameters (10).

Kinetic theory enables us to calculate a variety of gas properties from

the potential function $\Phi(r)$. The adequacy of the potential function

used to calculate the transport coefficients may be checked by investigat-

ing to what extent the same potential function reproduces other measured

properties of oxygen. Data for the second virial coefficient and the

thermal diffusion factor of oxygen are available for this purpose.

A.2 Second virial coefficient.

The second virial coefficient of a monatomic gas is given by the

expression

$$B = \frac{2}{3}\pi N\sigma^3 \int_0^\infty r^{\star 3} \frac{d\Phi\star}{dr\star} \exp\{-\Phi\star/T\star\}dr\star = \frac{2}{3}\pi N\sigma^3 B\star(T\star) \qquad (A1)$$

where $\Phi\star \equiv \Phi/\varepsilon$. Strictly speaking, this equation does not apply to a

polyatomic gas such as oxygen. Nevertheless, from tabulated values of

$B\star(T\star)$ for the m - 6 - 8 potential [45], we calculated the second virial

coefficient as a function of temperature using the potential parameters

(10) for oxygen. In Fig. 8 we have plotted the difference between the

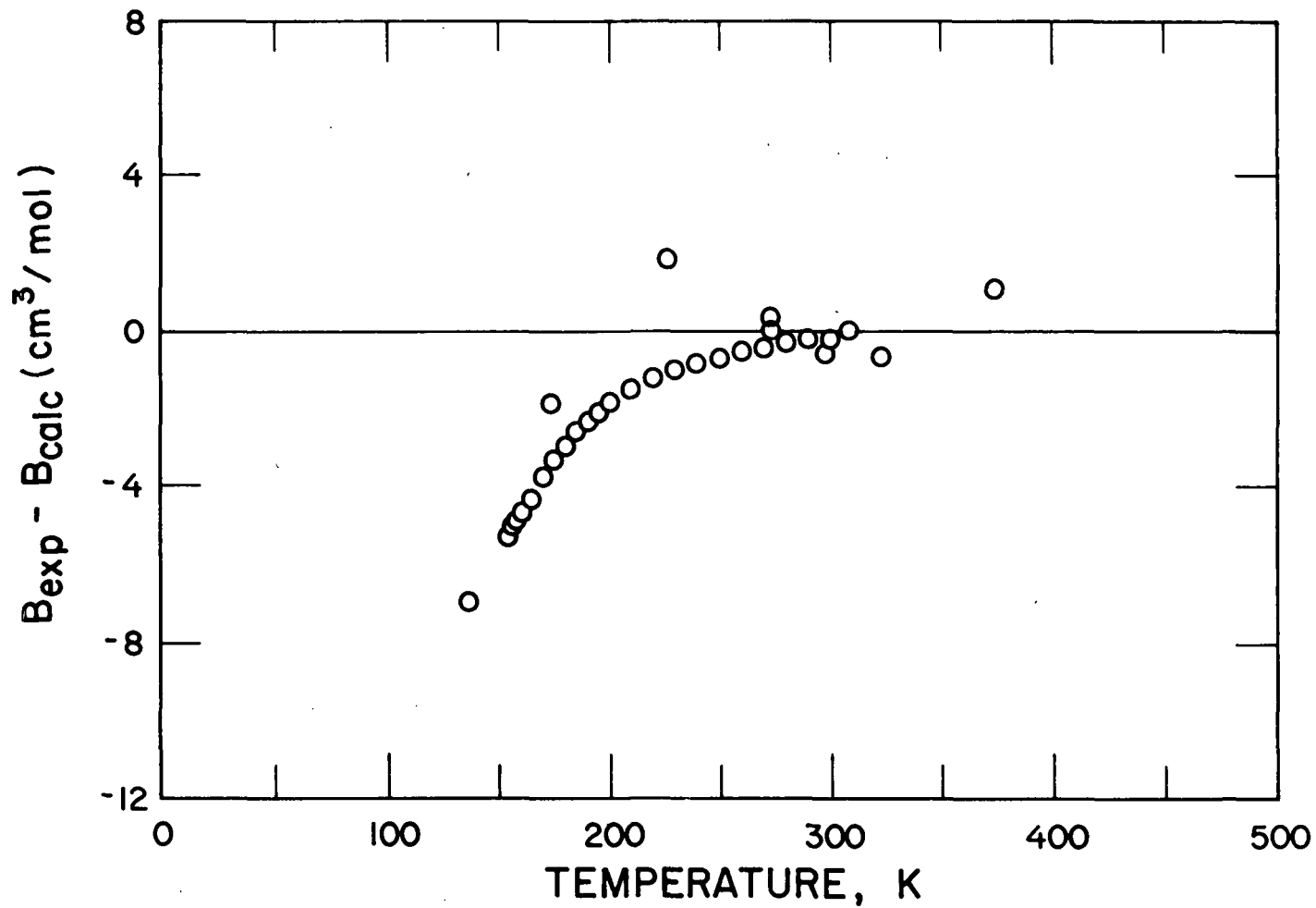experimental second virial coefficient data [66] and the values thus

Figure 8. Difference between experimental and calculated second virial coefficient of oxygen as a function of temperature. The experimental data are taken from ref. [66] and the theoretical values are calculated from equation (A1).

calculated. Although there is evidence of a definite systematic error, the result should be considered satisfactory, because it has been shown that the addition of nonspherical terms in (A1) will lead to an improvement in the representation of B [44]. Conversely, it is known that nonspherical contributions to the viscosity coefficient are small.

A.3 Thermal diffusion factor.

The thermal diffusion factor is known to be very sensitive to the potential function used to calculate the collision integrals. Conversely, if experimental data for the thermal diffusion factor are available, an important test of the validity of a chosen potential function is obtained by comparing experimental and calculated thermal diffusion factors.

The kinetic theory of gases yields the following expression for the thermal diffusion factor [38,39,67]

$$\alpha_o = \alpha_o'(1 + \delta) \qquad , \qquad (A2)$$

where

$$\alpha_o' = \frac{15(6C^* - 5)(2A^* + 5)}{2A^*(16A^* - 12D^* + 55)} \qquad , \qquad (A3)$$

and

$$\delta = \frac{(7-8E^*)}{9}\left[\frac{(175/4)-15D^*-30C^*}{7(6C^*-5)} + \frac{5-6C^*}{5+2A^*} + \frac{3(7-8E^*)}{14} + \right.$$

$$+ \frac{2A^*}{(35/4+7A^*+4F^*)}\left\{\frac{(35/4)-5D^*-6C^*}{5-6C^*} + \right.$$

$$\left.\left. + \frac{7(5-6C^*) + A^*(7-8E^*)}{2(5+2A^*)} \cdot \frac{(35/8) + 28A^*-6F^*}{21A^*}\right\}\right] \qquad . \qquad (A4)$$

The quantities A*, C*, D*, E*, and F* are related to the collision integrals $\Omega^{(\ell,s)*}$ defined in (6) by

$$A* = \Omega^{(2,2)*}/\Omega^{(1,1)*} \quad ,$$

$$C* = \Omega^{(1,2)*}/\Omega^{(1,1)*} \quad ,$$

$$D* = [5\Omega^{(1,2)*} - 4\Omega^{(1,3)*}]/\Omega^{(1,1)*} \quad , \tag{A5}$$

$$E* = \Omega^{(2,3)*}/\Omega^{(2,2)*} \quad ,$$

$$F* = \Omega^{(3,3)*}/\Omega^{(1,1)*} \quad .$$

In Fig. 9 a comparison is made between the experimental data for the thermal diffusion factor of oxygen obtained by Mathur and Watson [68] and the values calculated from (A2) using our potential function. The agreement is very satisfactory. We note especially that α_o is correctly predicted to change its sign at $T \approx 120K$.

We conclude that the m – 6 – 8 potential (9) with parameters (10) does yield a satisfactory representation of the transport properties of gaseous oxygen.
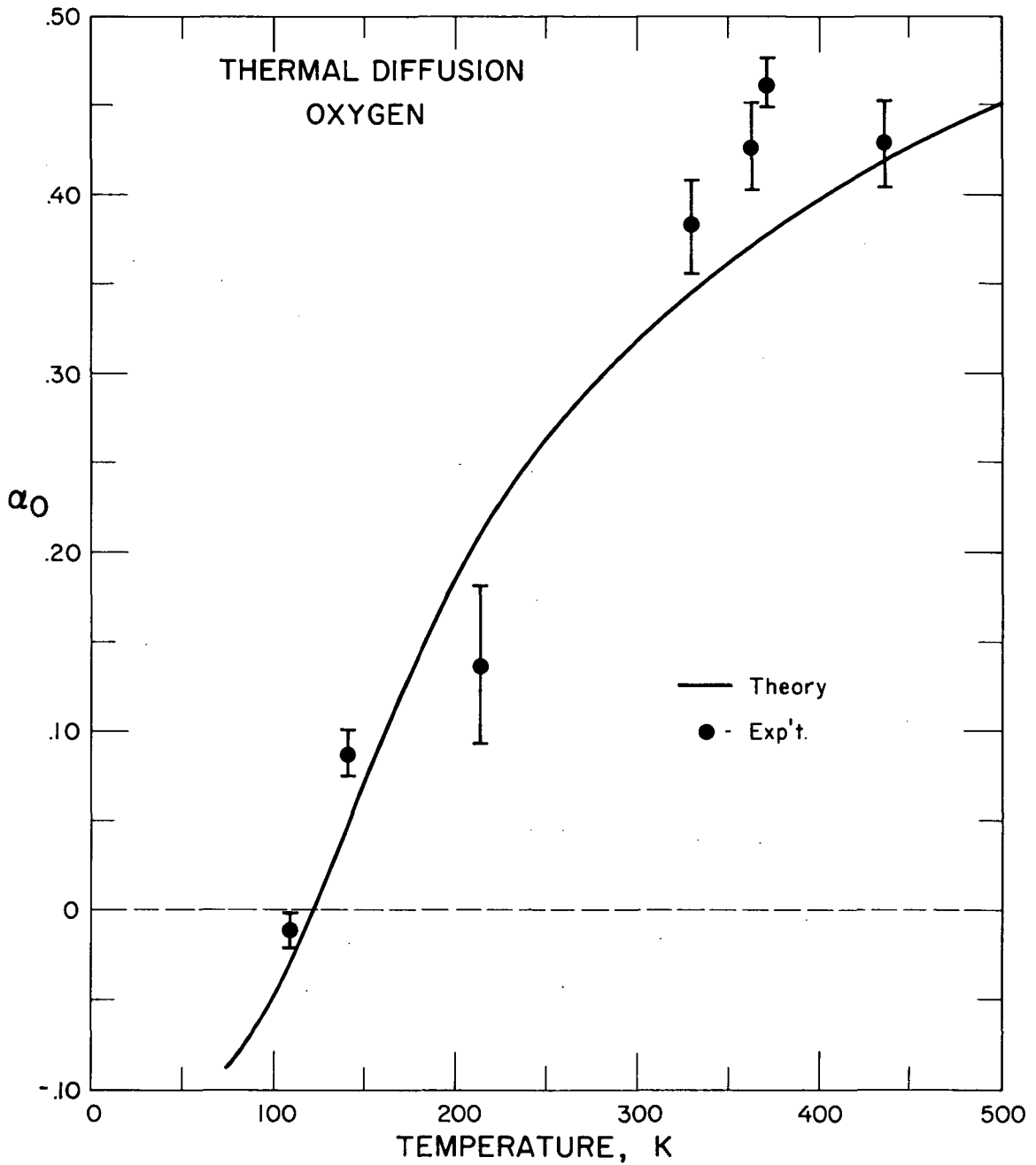
Figure 9. Isotopic thermal diffusion factor of oxygen as a function of temperature. The experimental data are taken from ref. [68] and the curve is calculated from equation (A2).

Appendix B

Critical enhancement of thermal conductivity.

B.1 Introduction.

In Section V we calculated the critical enhancement of the thermal conductivity for oxygen from equation (22). In order to justify the procedure we investigate in this Appendix to what extent this equation describes the thermal conductivity observed experimentally in the critical region of other fluids. The major source of information for this purpose is the set of thermal conductivity data for carbon dioxide in the critical region [69]. In addition we shall consider some limited information available for argon [70-72] nitrogen [70] and methane [73]. Some properties of these gases are listed in Table IX.

B.2 Carbon dioxide.

The thermal conductivity of compressed gases is written in this report as

$$\lambda(\rho,T) = \lambda_o(T) + \Delta\lambda(\rho) + \Delta_c\lambda(\rho,T) \qquad (B1)$$

where the critical enhancement $\Delta_c\lambda(\rho,T)$ is described by equation (22). This equation contains the short range correlation length R. For carbon dioxide this short range correlation length can be deduced from available light scattering [74] and X-ray scattering data [75]. From the X-ray scattering data of Chu and Lin we infer [2,54]

$$R = (4.0 \pm 0.2)\overset{\circ}{A} \left(\frac{\rho/\rho_c}{T/T_c} \right)^{1/2} \qquad (B2)$$

52

Table IX

Properties of CO_2, Ar, N_2 and CH_4

Parameters of m - 6 - 8 potential function [40]

fluid	m	γ	ϵ/k	σ	r_m
CO_2	14	1	282 K	3.680 Å	4.066 Å
Ar	11	3	153 K	3.292 Å	3.669 Å
N_2	12	2	118 K	3.54 Å	3.933 Å
CH_4	11	3	168 K	3.680 Å	4.101 Å

Critical parameters

fluid	T_c	ρ_c	P_c
CO_2	304.19 K	0.468 g/cm^3	72.785 atm
Ar	150.73 K	0.533 g/cm^3	47.983 atm
N_2	126.20 K	0.314 g/cm^3	33.56 atm
CH_4	190.77 K	0.162 g/cm^3	45.66 atm

53

In earlier publications we have referred to $\lambda_o(T) + \Delta\lambda$ in (B1) as the background thermal conductivity. An equation for $\Delta\lambda(\rho)$ was presented in ref. [54]. The critical enhancement $\Delta_c\lambda(\rho,T)$ of CO_2 can be calculated from equation (22) using the experimental value of R given in (B2), using the viscosity data of Kestin et al. [76] and using $(\partial P/\partial T)_\rho$ and K_T values deduced from the compressibility isotherms of Michels et al, [77].

Fig.10 shows the thermal conductivity of CO_2 in the critical region as a function of density and temperature. The various symbols represent experimental data points [69] and the curves represent the calculated values. A critical comparison very close to the critical point is hampered by some uncertainty in the knowledge of the critical temperature which was not measured during the thermal conductivity experiments. The agreement between experiment and theory at 31.2°C and 32.1°C can be improved by an appropriate adjustment of the value assumed for the critical temperature as was done in the previous technical report. Although the equation does not reproduce the observed in anomaly in complete detail, it yields a reasonable approximation and we prefer to use equation (22), because of its relative simplicity and its semi-theoretical connection with the mode coupling theory.

B.3 Other gases.

Detailed and reliable thermal conductivity data in the immediate vicinity of the critical point are presently limited to carbon dioxide. However, since the anomalous behavior of the thermal conductivity extends over a wide range of temperatures some experimental thermal conductivity data for other gases give also partial information concerning the
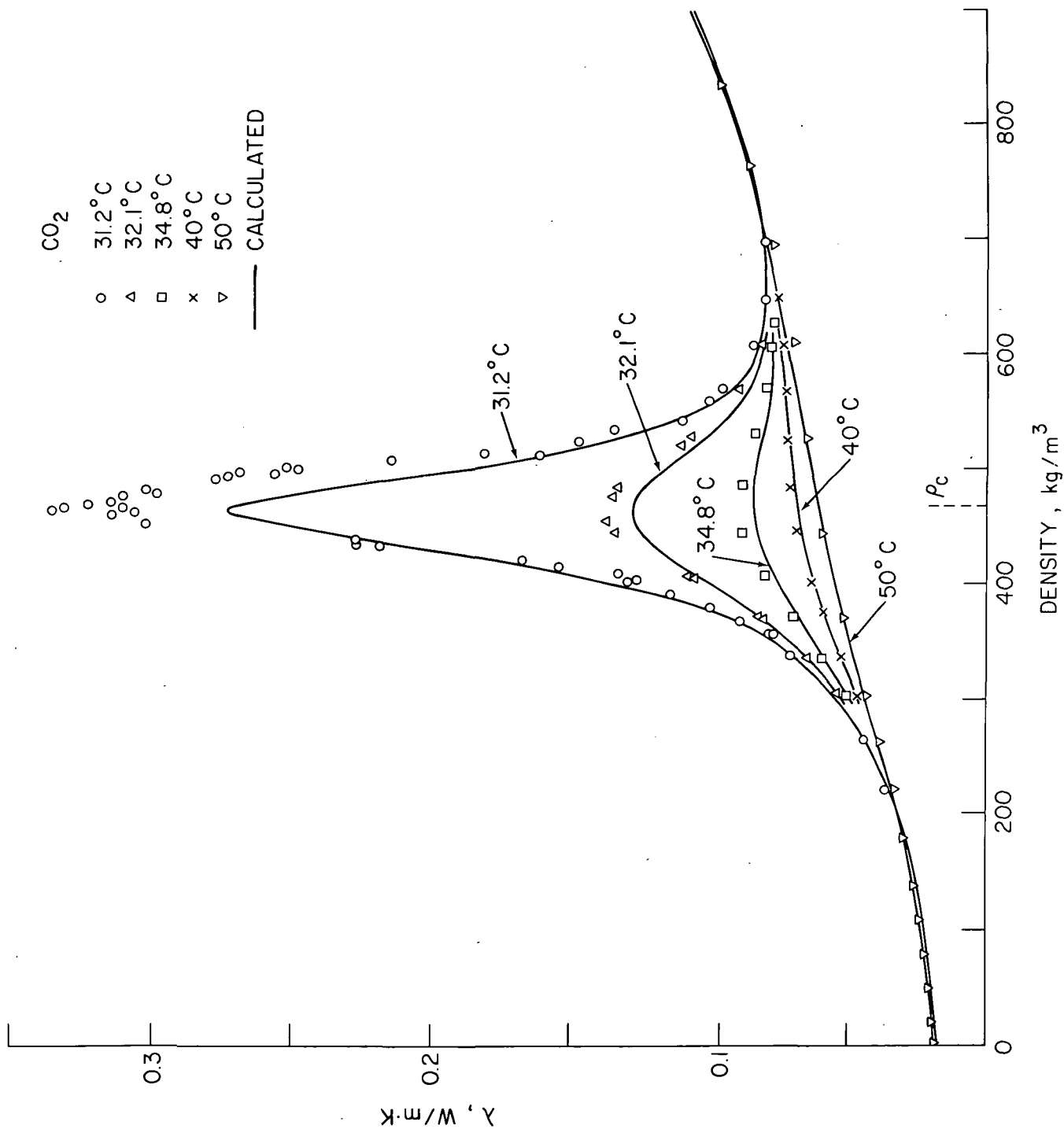
Figure 10. Thermal conductivity of carbon dioxide in the critical region as a function of density and temperature. The curves represent estimated values with the critical enhancement calculated from equations (22) and (B2).

anomaly [53,78].

Experimental data for the short range correlation length R of fluids as a function of density are scarce and of limited accuracy, the major source of information being the X-ray scattering data of Schmidt et al. for argon and nitrogen [79-81]. Therefore, we estimated the parameter R from the potential function via equation (25) proposed in the main text.

For the gases CO_2, Ar, N_2 and CH_4, R was thus calculated as a function of ρ/ρ_c using the potential function (9) with the appropriate parameters listed in Table IX. In Fig. 11 a comparison is made between the calculated values for R and experimental data[†] reported for argon [79], nitrogen [80] and carbon dioxide [75] near the critical temperature. In view of the limited precision as exemplified by the scatter in the experimental data, we consider equation (25) to yield a very satisfactory estimate of R. As mentioned in Section V, the assumption that the long range correlation length ℓ is symmetric around the critical density, implies R values proportional to $\sqrt{\rho}$ [††].

Having thus obtained estimated values for R we calculated the critical enhancement in the thermal conductivity from eq. (22) for CH_4, Ar and N_2. In selecting these gases we are guided by the condition that not only experimental thermal conductivity data but also reliable

---

[†] The short range correlation length ℓ reported by Schmidt et al. [79-81] is related to our parameter R by $R = \ell/\sqrt{10}$.

[††] We are indebted to J. S. Lin and P. W. Schmidt for informing us that their latest experimental X-ray scattering data near the critical point are consistent with this assumption.
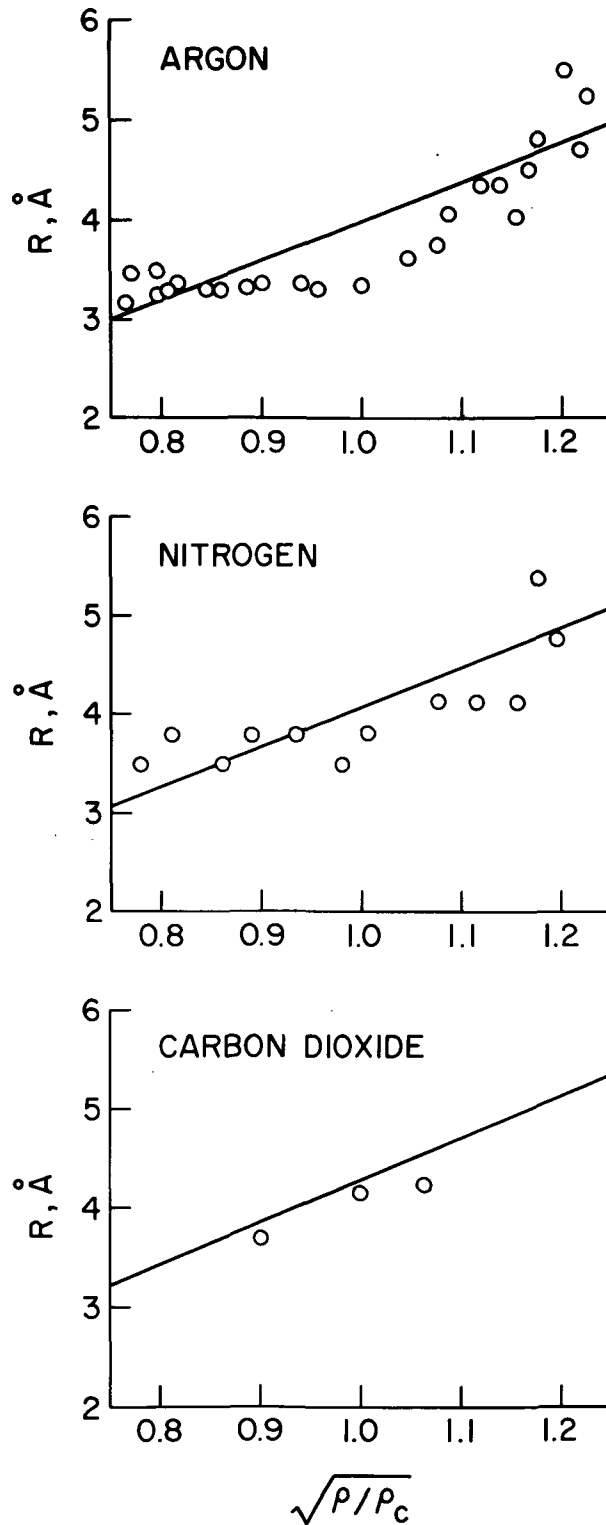
Figure 11. The short range correlation length R of argon, nitrogen and carbon dioxide near the critical temperature as a function of $\sqrt{\rho/\rho_c}$. The circles represent experimental data [75,79-81] and the line represents equation (25).

parameters for the potential function should be available [40].

We combine the critical enhancement $\Delta_c \lambda(\rho,T)$ with the temperature independent part $\Delta\lambda(\rho)$ of the excess background thermal conductivity to obtain the total excess thermal conductivity

$$\lambda(\rho,T) - \lambda_o(T) = \Delta\lambda(\rho) + \Delta_c\lambda(\rho,T) \tag{B3}$$

The excess function $\Delta\lambda(\rho)$ of these gases, as well as the viscosity to be substituted into (22) was obtained from an earlier report [82]. The equilibrium properties in (22) were calculated from Bender's equation of state [83]. The thermal conductivity was calculated at those temperatures where some experimental thermal conductivity data are available for comparison. Since these temperatures are not in the immediate vicinity of the critical point, use of Bender's equation should be adequate for the purpose at hand.

In Figs. 12 and 13 the total excess thermal conductivity is plotted as a function of density. The solid curve represents the excess background thermal conductivity $\Delta\lambda(\rho)$ and the dotted curves are obtained by adding the critical enhancement $\Delta_c\lambda(\rho,T)$ as calculated from equations (22) and (25). For methane a comparison can be made with experimental thermal conductivity cf Mani and Venart [73] and with a few data points of Ikenberry and Rice [71]. A similar comparison for argon is complicated by the fact that the available experimental data [70-72] show appreciable scatter. The corresponding information for nitrogen is presented in Table X, where only three experimental data points of Ziebland and Burton [70,78] are available for comparison. From the
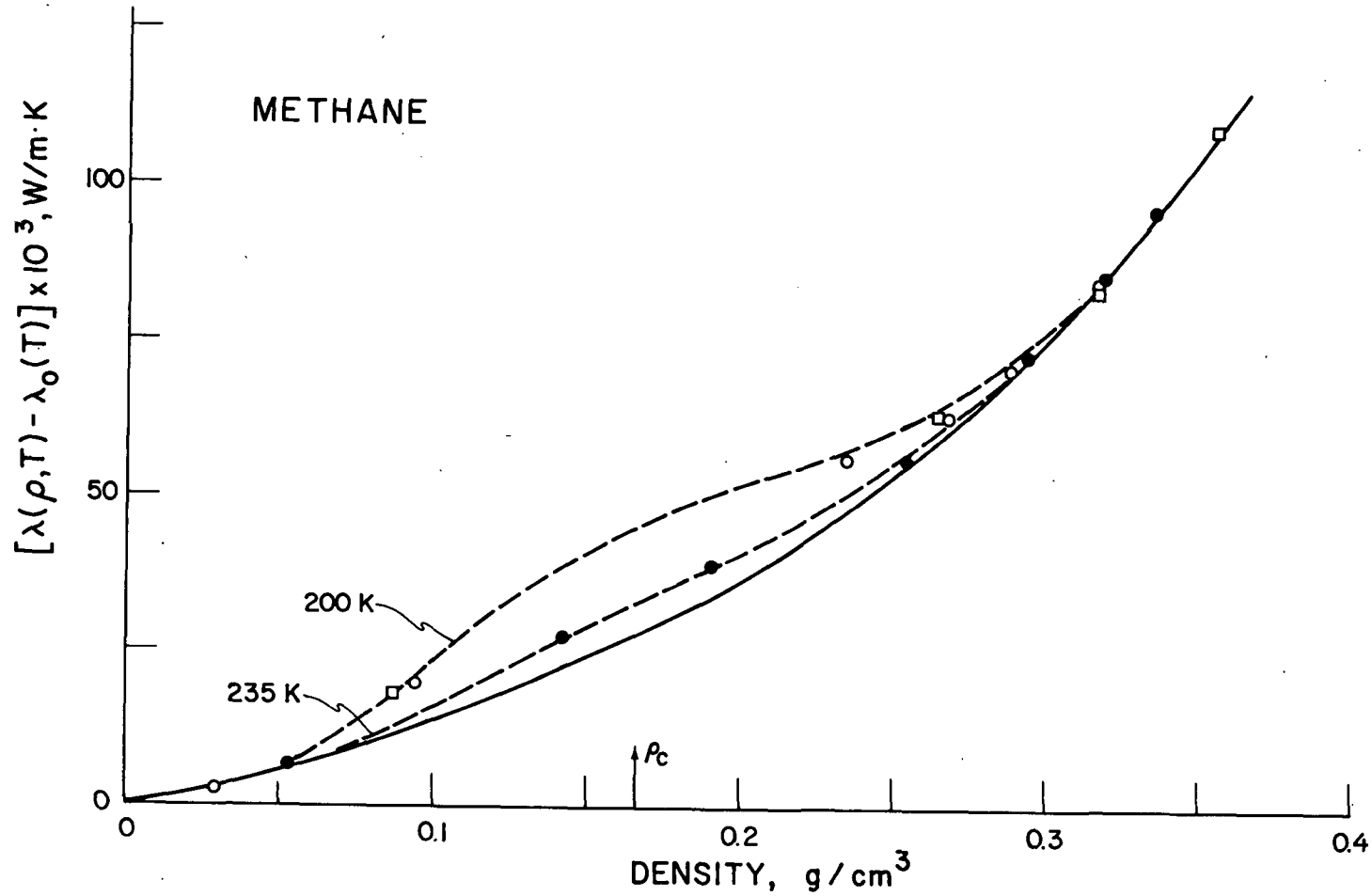
Figure 12. Total excess thermal conductivity $\lambda(\rho,T) - \lambda_o(T)$ of methane in the critical region. The solid line represents the background thermal conductivity and the dashed lines represent the anomalous thermal conductivity as predicted from equation (22). Data: □ 200K [73], 0 200K [71], 0 235K [71].

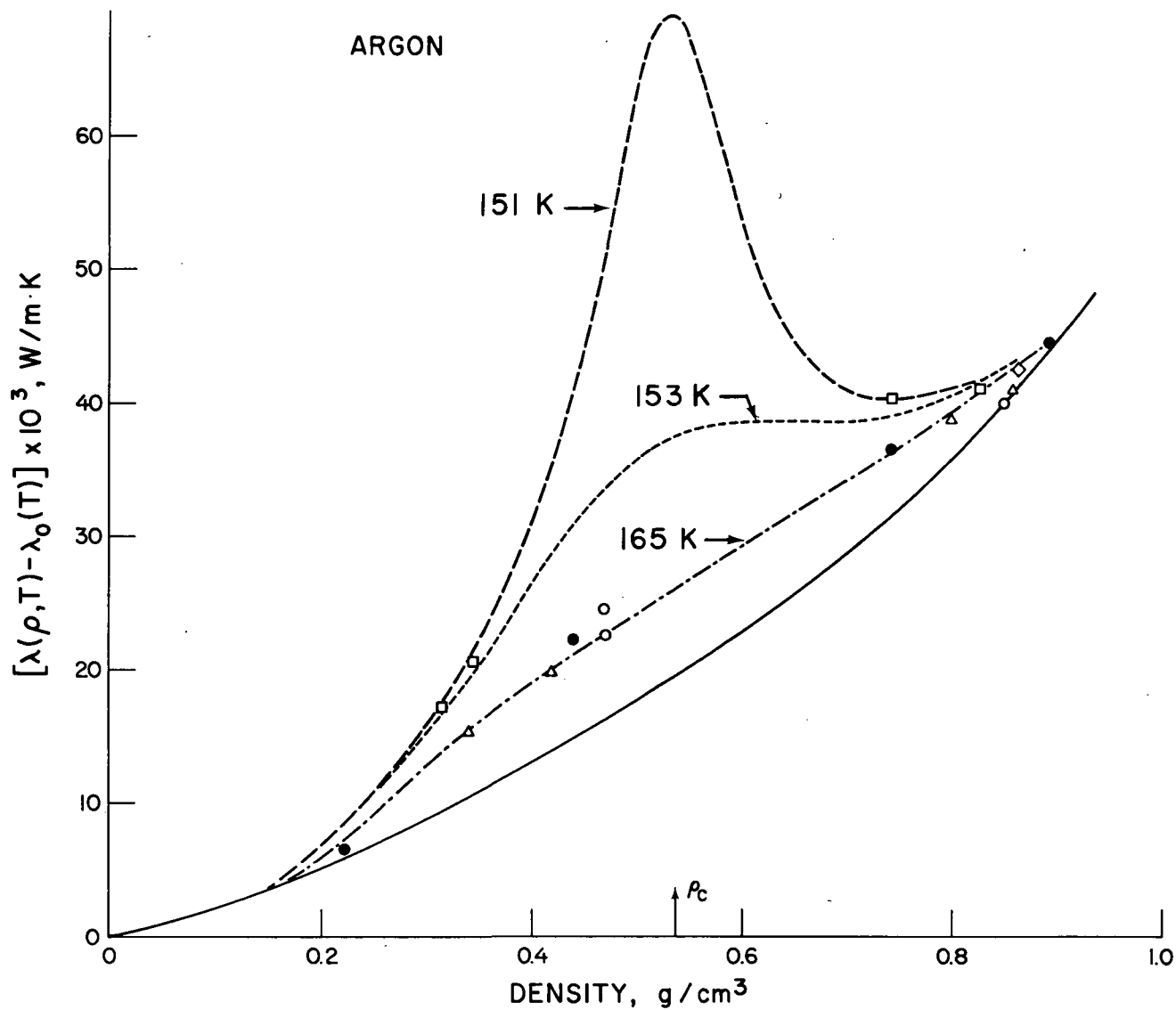Figure 13. Total excess thermal conductivity $\lambda(\rho,T) - \lambda_o(T)$ of argon in the critical region. The solid line represents the background thermal conductivity and the dashed lines represent the anomalous thermal conductivity as predicted from equation (22), Data: ⊔ 151K [72], ◇ 152K [70], o 165K [70], ● 165K [71], Δ 165K [72].

information in Figs. 11, 12, 13 and in Table X we conclude that our equation does yield an adequate representation of the thermal conductivity in the critical region of fluids.

Table X.

Comparison between experimental and calculated values for the total excess thermal conductivity $\lambda(\rho,T) - \lambda_o(T)$ of nitrogen in the critical region. Experimental data from ref. [70].

Density g/cm^3	Temperature K	$\Delta\lambda(\rho)$ milliwatt/m.K	$\Delta\lambda(\rho) + \Delta_c\lambda(\rho,T)$ milliwatt/m.K	
			exp	calc
0.255	139.0	14.9	21.8	21.9
0.291	136.9	18.2	24.4	26.7
0.314	136.2	20.2	32.4	30.2

REFERENCES

1. J. V. Sengers, *Transport Properties of Compressed Gases*, in Recent Advances in Engineering Science, Vol. III, A. C. Eringen, ed. (Gordon and Breach, New York, 1968), p. 153.

2. J. V. Sengers, *Transport Properties of Gases and Binary Liquids Near the Critical Point*, NASA Contractor Report NASA CR-2112 (National Aeronautics and Space Administration, Washington, D. C., 1972).

3. R. Wobser and F. Müller, *The Viscosity of Gas Vapors and Their Measurements in a Hoppler Viscometer*, Kolloid Beih. 52, 165 (1941).

4. J. Kestin and W. Leidenfrost, *An Absolute Determination of the Viscosity of Eleven Gases Over a Range of Pressures*, Physica 25, 1033 (1959).

5. L. Andrussow, *Thermal Conductivity, Viscosity and Diffusion in the Gas Phase*, J. Chim. phys. 52, 295 (1955).

6. J. Van Lierde, *Measurements of Thermal Diffusion and Viscosity of Certain Gas Mixtures at Low and Very Low Temperatures*, Verhandel. Koninkl. Vlaamse Acad. Wetenschappen, Belgie Kl. Wetenschap. (24) 9, 7 (1947).

7. H. L. Johnston and K. E. McCloskey, *Viscosities of Several Common Gases Between 90K and Room Temperature*, J. Phys. Chem. 44, 1038 (1940).

8. M. Trautz and A. Melster, *The Viscosity of H_2, N_2, CO, C_2H_4, O_2 and Their Binary Mixtures*, Ann. Physik 399, 409 (1930); M. Trautz and R. Heberling, *The Viscosity of NH_3 and Its Mixtures with H_2, N_2,*

O_2, C_2H_4, Ann. Physik <u>402</u>, 155 (1931); M. Trautz and H. Zimmerman, *The Viscosity of Hydrogen, Helium and Neon and Their Binary Mixtures at Low Temperatures*, Ann. Physik <u>414</u>, 189 (1935).

9. C. J. G. Raw and C. P. Ellis, *High-Temperature Gas Viscosities. I. Nitrous Oxide and Oxygen*, J. Chem. Phys. <u>28</u>, 1198 (1958).

10. A. Van Itterbeek and A. Claes, *Measurements of the Viscosity of Gaseous Oxygen at Low Temperatures*, Physica <u>3</u>, 275 (1936).

11. J. Kestin, W. Wakeham and K. Watanabe, *Viscosity, Thermal Conductivity, and Diffusion Coefficient of Ar-Ne and Ar-Kr Gaseous Mixtures in the Temperature Range 25-700°C*; R. DiPippo and J. Kestin, *The Viscosity of Seven Gases up to 500°C and Its Statistical Interpretation*, in Proc. 4th Symposium on Thermophysical Properties, J. R. Moszynski, ed. (American Society of Mechanical Engineers, New York, 1968), p. 304.

12. A. G. Clarke and E. B. Smith, *Low-Temperature Viscosities of Argon, Krypton and Xenon*, J. Chem. Phys. <u>48</u>, 3988 (1968); R. A. Dawe and E. B. Smith, *Viscosities of the Inert Gases at High Temperatures*, J. Chem. Phys. <u>52</u>, 693 (1970); R. A. Dawe, G. C. Maitland, M. Rigby and E. B. Smith, *High Temperature Viscosities and Intermolecular Forces of Quasi-spherical Molecules*, Trans. Farad. Soc. <u>66</u>, 1955 (1970).

13. F. A. Guevara, B. B. McInteer and W. E. Wageman, *High-Temperature Viscosity Ratios for Hydrogen, Helium, Argon, and Nitrogen*, Phys. Fluids <u>12</u>, 2493 (1969); M. Goldblatt, F. A. Guevara and B. B. McInteer, *High Temperature Viscosity Ratios for Krypton*, Phys.

Fluids *13*, 2873 (1970); M. Goldblatt and W. E. Wageman, *High Temperature Viscosity Ratios for Xenon*, Phys. Fluids *14*, 1024 (1971).

14. H. J. M. Hanley and G. E. Childs, *Discrepancies Between Viscosity Data for Simple Gases*, Science *159*, 1114 (1968).

15. M. Trautz and R. Zink, *Viscosity of Gases at High Temperatures*, Ann. Physik *399*, 427 (1930).

16. H. L. Johnston and E. R. Grilly, *Viscosities of CO, He, Ne, and Ar Between 80 and 300 K. Coefficients of Viscosity*, J. Phys. Chem. *46*, 948 (1942).

17. A. Eucken, *On the Temperature Dependence of the Thermal Conductivity of Several Gases*, Physik. Z. *12*, 1101 (1911).

18. H. Geier and K. Schäfer, *Heat Conductivity of Pure Gases and Gas Mixtures at 0-1200°*, Allgem. Wärmetechn. *10*, 70 (1961).

19. E. U. Franck, *Thermal Conductivity in Gases at High Pressures*, Chem. Eng. Techn. *25*, 238 (1953).

20. H. Gregory and S. Marshall, *The Thermal Conductivities of Oxygen and Nitrogen*, Proc. Roy. Soc. (London) *A118*, 594 (1928).

21. W. G. Kannuluik and L. H. Martin, *The Thermal Conductivity of Some Gases at 0°C*, Proc. Roy. Soc. (London) *A144*, 496 (1934).

22. W. Nothdurft, *Absolute Determination of the Thermal Conductivity of Gases*, Ann. Physik *420*, 137 (1937).

23. H. L. Johnston and E. R. Grilly, *The Thermal Conductivity of Eight Common Gases Between 80 and 380 K*, J. Chem. Phys. *14*, 233 (1946).

24. N. V. Tsederberg and D. L. Timrot, *An Experimental Determination of the Thermal Conductivity of Liquid Oxygen*, Soviet Phys. Techn. Phys. *1*, 1791 (1956) [translated from Zhur. Tekh. Fiz. *26*, 1849 (1956)].

25. H. Cheung, *Thermal Conductivity and Viscosity of Gas Mixtures*, Report No. UCRL-8230 (Lawrence Radiation Lab., Univ. California, 1958).

26. A. N. G. Pereira and C. J. G. Raw, *Heat Conductivities of Poly-atomic Gases and Their Binary Mixtures*, Phys. Fluids <u>6</u>, 1091 (1963).

27. A. A. Westenberg and N. De Haas, *Gas Thermal Conductivity Studies at High Temperature. II. Results for O_2 and O_2-H_2O Mixtures*, Phys. Fluids <u>6</u>, 617 (1963).

28. N. S. Rudenko and L. N. Shubnikov, *Viscosity of Liquid N_2, CO, Ar and O_2 and Its Dependence on Temperature*, Physik. Z. Sowjetunion <u>6</u>, 470 (1934).

29. J. P. Boon and G. Thomaes, *The Viscosity of Liquefied Gases*, Physica <u>29</u>, 208 (1963).

30. W. Grevendonk, W. Herreman, W. De Pesseroey and A. De Bock, *On the Shear Viscosity of Liquid Oxygen*, Physica <u>40</u>, 207 (1968).

31. R. Kiyama and T. Makita, *An Improved Viscometer for Compressed Gases and the Viscosity of Oxygen*, Rev. Phys. Chem. Japan <u>26</u>. 70 (1956).

32. H. Ziebland and J. T. A. Burton, *The Thermal Conductivity of Liquid and Gaseous Oxygen*, Brit. J. Appl. Phys. <u>6</u>, 416 (1953).

33. Z. A. Ivanova, N. V. Tsederberg and V. N. Popov, *Experimental Study of Thermal Conductivity of Oxygen*, Teploenergetika <u>14</u> (10), 74 (1967).

34. G. E. Childs and H. J. M. Hanley, *The Viscosity and Thermal Con-ductivity Coefficients of Dilute Nitrogen and Oxygen*, NBS Technical Note 350 (U. S. Govt. Printing Office, Washington, D. C., 1966).

35. C. Y. Ho, R. W. Powell and P. E. Liley, *Thermal Conductivity of the Elements*, J. Phys. Chem. Ref. Data $\underline{1}$, 279 (1972).

36. G. C. Maitland and E. B. Smith, *Critical Reassessment of Viscosities of 11 Common Gases*, J. Chem. Eng. Data $\underline{17}$, 150 (1972).

37. A. A. Vasserman, Ya. Z. Kazavchinskii and V. A. Rabinovich, *Thermophysical Properties of Air and Air Components* (Akad. Nauk SSSR, Moscow, 1966; translation: Israel Program for Scientific Translations, Jerusalem, 1971).

38. S. Chapman and T. G. Cowling, *The Mathematical Theory of Non-Uniform Gases*, 3rd ed. (Cambridge Univ. Press, London, 1970).

39. J. O. Hirschfelder, C. F. Curtiss and R. B. Bird, *Molecular Theory of Gases and Liquids* (John Wiley, New York, 1954), p. 527.

40. H. J. M. Hanley and M. Klein, *Application of the m-6-8 Potential to Simple Gases*, J. Phys. Chem. $\underline{76}$, 1743 (1972).

41. E. A. Mason and L. Monchick, *Heat Conductivity of Polyatomic and Polar Gases*, J. Chem. Phys. $\underline{36}$, 1622 (1962); E. A. Mason, *Prediction of Transport Coefficients of Dilute Gases*, in Proc. 4th Symposium on Thermophysical Properties, J. R. Moszynski, ed. (American Society of Mechanical Engineers, New York, 1968), p. 21.

42. M. Klein and H. J. M. Hanley, *m-6-8 Potential Function*, J. Chem. Phys. $\underline{53}$, 4722 (1970).

43. H. J. M. Hanley and M. Klein, *On the Utility of the m-6-8 Potential Function*, NBS Technical Note 628 (U. S. Govt. Printing Office, Washington, D. C., 1972).

44. J. F. Ely and H. J. M. Hanley, *Analysis of the Viscosity and Second Virial Coefficients of Non-polar Polyatomic Gases Using the m-6-8 Potential*, Mol. Phys. $\underline{24}$, 683 (1972).

45. M. Klein, F. J. Smith, H. J. M. Hanley and P. M. Holland, *Tables of Collision Integrals and Second Virial Coefficients for the (m,6,8) Intermolecular Potential Function*, NSRD Monograph No. 47 (U. S. Govt. Printing Office, Washington, D. C., 1973).

46. H. W. Woolley, *Thermodynamic Functions for Molecular Oxygen in the Ideal Gas State*, J. Res. NBS <u>40</u>, 163 (1948).

47. G. Ganzi and S. I. Sandler, *Determination of Thermal Transport Properties from Thermal Transpiration Measurements*, J. Chem. Phys. <u>55</u>, 132 (1971).

48. D. E. Diller, H. J. M. Hanley and H. M. Roder, *The Density and Temperature Dependence of the Viscosity and Thermal Conductivity of Dense Simple Fluids*, Cryogenics <u>10</u>, 286 (1970).

49. H. J. M. Hanley, R. D. McCarty and J. V. Sengers, *Density Dependence of Experimental Transport Coefficients of Gases*, J. Chem. Phys. <u>50</u>, 857 (1969).

50. J. Kestin, E. Paykoç and J. V. Sengers, *On the Density Expansion for Viscosity in Gases*, Physica <u>54</u>, 1 (1971).

51. R. B. Stewart, R. T. Jacobsen and A. F. Myers, *The Thermodynamic Properties of Oxygen and Nitrogen, Part II*, Final Report on Contract NAS 9-12078 (Engineering Experiment Station, Univ. Idaho, Moscow, Idaho, 1972); R. T. Jacobsen, R. B. Stewart and A. F. Myers, *An Equation of State for Oxygen and Nitrogen*, Advances in Cryogenic Engineering, Vol. 18, K. D. Timmerhaus, ed. (Plenum Press, New York, 1973), p. 248.

52. J. V. Sengers, *Transport Properties of Gases and Binary Liquids Near the Critical State*, in Transport Phenomena – 1973, AIP

Conference Proceedings No. 11, J. Kestin, ed. (American Institute of Physics, New York, 1973), p. 229.

53. J. V. Sengers, *Transport Properties of Fluids Near Critical Points*, in Proc. Intern. School "Enrico Fermi," Course LI, M. S. Green, ed. (Academic Press, New York, 1971), p. 445.

54. J. V. Sengers, *Transport Processes Near the Critical Point of Gases and Binary Liquids in the Hydrodynamic Regime*, Ber. Bunsenges. phys. Chem. <u>76</u>, 234 (1972).

55. B. Le Neindre, R. Tufeu, P. Bury and J. V. Sengers, *Thermal Conductivity of Carbon Dioxide and Steam in the Supercritical Region*, Ber. Bunsenges. phys. Chem. <u>77</u>, 262 (1973).

56. R. C. Hendricks and A. Baron, *Prediction of the Thermal Conductivity Anomaly of Simple Substances in the Critical Region*, Paper 71-HT-28 (Heat Transfer Division, American Society of Mechanical Engineers, New York, 1971).

57. R. S. Brokaw, *Statistical Mechanical Theories of Transport Properties*, NASA TM X-52478 (National Aeronautics and Space Administration, Washington, D. C., 1968).

58. M. E. Fisher, *Correlation Functions and the Critical Region of Simple Fluids*, J. Math. Phys. <u>6</u>, 944 (1964).

59. M. Vicentini-Missoni, J. M. H. Levelt Sengers and M. S. Green, *Scaling Analysis of Thermodynamic Properties in the Critical Region of Fluids*, J. Res. NBS <u>73A</u>, 563 (1969).

60. J. M. H. Levelt Sengers, *Scaling Predictions for Thermodynamic Anomalies Near the Gas-Liquid Critical Point*, Ind. Eng. Chem. Fundam. <u>9</u>, 470 (1970).

68

61. A. Münster, *Basic Concepts and Problems in the Theory of Critical Phenomena*, Ber. Bunsenges. phys. Chem. <u>76</u>, 185 (1972).

62. J. S. Rowlinson, *The Thermodynamics of the Critical Point in One-Component Systems*, Ber. Bunsenges. phys. Chem. <u>76</u>, 281 (1972).

63. J. M. H. Levelt Sengers, W. L. Greer and J. V. Sengers, *Scaled Parametric Equation-of-State for Oxygen in the Critical Region*, Advances in Cryogenic Engineering, Vol. 19, K. D. Timmerhaus, ed.

64. R. D. McCarty and L. A. Weber, *Thermophysical Properties of Oxygen from the Freezing Liquid Line to 600 R for Pressures to 5000 Psi*, NBS Technical Note 384 (U. S. Govt. Printing Office, Washington, D. C., 1971).

65. H. M. Roder and L. A. Weber, *ASRDI Oxygen Technological Survey, Vol. I: Thermophysical Properties*, NASA SP-3071 (National Aeronautics and Space Administration, Washington, D. C., 1972).

66. L. A. Weber, *P-V-T, Thermodynamic and Related Properties of Oxygen from the Triple Point to 300K at Pressures to 33 MN/m^2*, J. Res. NBS <u>74A</u>, 93 (1970).

67. H. J. M. Hanley and M. Klein, *Selection of the Intermolecular Potential Function. III. From the Isotopic Thermal Diffusion Factor*, J. Chem. Phys. <u>50</u>, 4765 (1969).

68. B. P. Mathur and W. W. Watson, *Thermal Diffusion in Isotopic $^{16}O_2 - {}^{18}O_2$*, J. Chem. Phys. <u>51</u>, 2210 (1969).

69. A. Michels, J. V. Sengers and P. S. Van der Gulik, *The Thermal Conductivity of Carbon Dioxide in the Critical Region. II. Measurements and Conclusions*, Physica <u>28</u>, 1216 (1962).

70. H. Ziebland and J. T. A. Burton, *The Thermal Conductivity of Nitrogen and Argon in the Liquid and Gaseous States*, Brit. J. Appl. Phys. 9, 52 (1958).

71. L. D. Ikenberry and S. A. Rice, *Experimental and Theoretical Studies of Thermal Conductivity in Liquid Ar, Kr, Xe and CH_4*, J. Chem. Phys. 39, 1561 (1963).

72. B. J. Bailey and K. Kellner, *The Thermal Conductivity of Liquid and Gaseous Argon*, Physica 39, 444 (1968).

73. N. Mani and J. S. S. Venart, *Thermal Conductivity Measurements of Liquid and Dense Gaseous Methane*, Advances in Cryogenic Engineering, Vol. 18, K. D. Timmerhaus, ed. (Plenum Press, New York, 1973), p. 280; N. Mani, *Precise Determination of the Thermal Conductivity of Fluids using Absolute Transient Hot-Wire Technique*, Ph. D. Thesis (Univ. Calgary, Calgary, Alberta, Canada, 1971).

74. B. S. Maccabee and J. A. White, *Supercritical Correlation Length of Carbon Dioxide along the Critical Isochore*, Phys. Rev. Letters 27, 495 (1971).

75. B. Chu and J. S. Lin, *Small-Angle Scattering of X Rays from Carbon Dioxide in the Vicinity of its Critical Point*, J. Chem. Phys. 53, 4454 (1970).

76. J. Kestin, J. H. Whitelaw and T. F. Zien, *The Viscosity of Carbon Dioxide in the Neighbourhood of the Critical Point*, Physica 30, 161 (1964).

77. A. Michels and C. Michels, *Isotherms of CO_2 between 0° and 150°C and Pressures from 16 to 250 Atm.*, Proc. Roy. Soc. (London) A153 201 (1935); A. Michels, C. Michels and H. Wouters, *Isotherms of*

CO_2 *between 70 and 3000 Atm.,* Proc. Roy. Soc. (London) <u>A153</u>,

214 (1935); A. Michels, B. Blaisse and C. Michels, *The Isotherms*

of CO_2 in the Neighbourhood of the Critical Point and Round the

Coexistence Line, Proc. Roy. Soc. (London) <u>A160</u>, 358 (1937).

78. J. V. Sengers, *Thermal Conductivity and Viscosity of Simple*

Fluids, Intern. J. Heat Mass Transfer <u>8</u>, 1103 (1965).

79. J. S. Thomas and P. W. Schmidt, *X-Ray Study of Critical Opalescence*

in Argon, J. Chem. Phys. <u>39</u>, 2506 (1963).

80. J. E. Thomas and P. W. Schmidt, *A Small-Angle X-Ray Scattering*

Study of Critical Opalescence in Nitrogen, J. Am. Chem. Soc. <u>86</u>,

3554 (1964).

81. P. W. Schmidt and C. W. Tompson, *X-Ray Scattering Studies of*

Simple Fluids, in Simple Dense Fluids, H. L. Frisch and Z. W.

Salsburg, eds. (Academic Press, New York, 1968), p. 31.

82. P. E. Angerhofer and H. J. M. Hanley, *The Viscosity and Thermal*

Conductivity Coefficients of Nine Fluids: Preliminary Values,

NBS Report 10700 (National Bureau of Standards, Boulder, Colo.,

1971).

83. E. Bender, *Equations of State Exactly Representing the Phase*

Behavior of Pure Substances, in Proc. 5th Symposium on Thermo-

physical Properties, C. F. Bonilla, ed. (American Society of

Mechanical Engineers, New York, 1970). p. 227.